



Research paper

Phthalimido-thiazoles as building blocks and their effects on the growth and morphology of *Trypanosoma cruzi*

Paulo André Teixeira de Moraes Gomes^a, Arsênio Rodrigues Oliveira^a,
 Marcos Veríssimo de Oliveira Cardoso^a, Edna de Farias Santiago^a,
 Miria de Oliveira Barbosa^a, Lucianna Rabelo Pessoa de Siqueira^a,
 Diogo Rodrigo Magalhães Moreira^b, Tanira Matutino Bastos^b, Fábio André Brayner^c,
 Milena Botelho Pereira Soares^{b,d}, Andresa Pereira de Oliveira Mendes^e,
 Maria Carolina Accioly Brelaz de Castro^e, Valéria Rego Alves Pereira^e,
 Ana Cristina Lima Leite^{a,*}

^a Departamento de Ciências Farmacêuticas, Centro de Ciências da Saúde, Universidade Federal de Pernambuco, 50740-520 Recife, PE, Brazil

^b Fundação Oswaldo Cruz, Centro de Pesquisas Gonçalo Moniz, CEP 40296-710 Salvador, BA, Brazil

^c Laboratório de Imunologia Keizo Asami-LIKA/UFPE, CEP, 50670-901 Recife, PE, Brazil

^d Centro de Biotecnologia e Terapia Celular, Hospital São Rafael, Avenida São Rafael, 2152, São Marcos, CEP 41253-190, Salvador BA, Brazil

^e Centro de Pesquisas Aggeu Magalhães, Fundação Oswaldo Cruz, CEP, 50670-420 Recife, PE, Brazil

ARTICLE INFO

Article history:

Received 21 September 2015

Received in revised form

21 December 2015

Accepted 9 January 2016

Available online 11 January 2016

Keywords:

Chagas disease

Trypanosoma cruzi

Thiazole

Hydrazone

Phthalimide

ABSTRACT

Chagas disease is a parasitic infection caused by protozoan *Trypanosoma cruzi* that affects approximately 6–7 million people worldwide. Benznidazole is the only drug approved for treatment during the acute and asymptomatic chronic phases; however, its efficacy during the symptomatic chronic phase is controversial. The present work reports the synthesis and anti-*T. cruzi* activities of a novel series of phthalimido-thiazoles. Some of these compounds showed potent inhibition of the trypanostigote form of the parasite at low cytotoxicity concentrations in spleen cells, and the resulting structure-activity relationships are discussed. We also showed that phthalimido-thiazoles induced ultrastructural alterations on morphology, flagellum shortening, chromatin condensation, mitochondria swelling, reservosomes alterations and endoplasmic reticulum dilation. Together, these data revealed, for the first time, a novel series of phthalimido-thiazoles-structure-based compounds with potential effects against *T. cruzi* and lead-like characteristics against Chagas disease.

© 2016 Elsevier Masson SAS. All rights reserved.

1. Introduction

Chagas disease, also known as American trypanosomiasis, is a potentially life-threatening illness caused by the protozoan parasite *Trypanosoma cruzi* (*T. cruzi*). Approximately 6–7 million people are estimated to be infected worldwide, mostly in Latin America, where Chagas disease is endemic [1].

Despite the efforts of many investigators to research new anti-Chagas drugs, only one drug is currently used in therapy, benznidazole (Bdz) [2,3]. Current chemotherapy for Chagas disease is unsatisfactory due to the limited efficacy of Bdz, particularly during

the chronic phase, with frequent side effects that can lead to discontinuation of treatment [4].

One pragmatic way to improve the quality of both the candidate drugs and screening collections is by improving the quality of the building blocks (reagents) that are used to synthesize them. Our strategic program focused on substructures and properties that are known to have imparted biological activity and good ‘drug-like’ properties previously. Among the chemical groups explored for anti-Chagas activity, thiazolyl hydrazones are noteworthy because of their wide biological, especially anti-parasitic, activities [5–8]. Caputo et al. have demonstrated trypanocidal activity for a series of 4-arylthiazolylhydrazones [9], which have broad and potent activities for all forms of the parasite.

Our efforts toward new antichagasic drugs since 2006 have led

* Corresponding author.

E-mail address: acllb2003@yahoo.com.br (A.C.L. Leite).

us to develop a variety of thiosemicarbazones and 1,3-thiazolyl hydrazones as trypanocidal agents [4,7,10–14]. In continuation of our search for bioactive molecules, we envisaged that the derivatization of the thiosemicarbazone group into a thiazole moiety would generate novel templates that are likely to exhibit anti-*T. cruzi* activity [4].

However, much effort has been invested to identify the key differences between drugs and other organic compounds. High-quality libraries are expected to exhibit drug-likeness to produce compounds with desirable pharmacokinetic and safety profiles. The phthalimide functional group has been used as an important tool in organic synthesis because it protects against unwanted reactions. Many research teams have used this nucleus as a building block to improve compound quality. In fact, phthalimide derivatives have shown a broad spectrum of pharmacological properties, such as analgesic [15], anticonvulsant [16], antitubercular [17,18], hypolipidaemic [18], anxiolytic [15], anti-inflammatory [15], antimicrobial [17,19,20] and antipsychotic [21].

For this reason, our research group has explored the pharmacological properties of phthalimide derivatives. As a result, bioactive prototypes were identified with potent anti-inflammatory [22], anti-proliferative [23], immunomodulatory [22,24,25], antitumor [23], antiangiogenic [26] and schistosomicidal properties [27]. Indeed, Santiago et al. identified phthalimido-thiazole derivatives with potent schistosomicidal activities. The phthalimide **LpQM-45** caused significant ultrastructural changes, including destruction of the integument in both male and female worms [27], however, their antichagasic properties have not been explored.

Considering the promising results achieved by compounds bearing a thiazole ring and phthalimides nuclei, they were chosen as common pharmacophores that exist in diverse drug classes. In this way, we synthesized a set of molecules with phthalimide and thiazole nucleus. In this synthetic design of a substructure-based compound library, substituents around the phenyl ring attached at C4 in the thiazole ring (compounds **2b-n**) were explored. In addition, a spacer group between phthalimide and the thiazole ring was inserted and a phenyl group at N3 of the thiazole ring was also introduced (**6b-l**). To investigate the influence of the phthalimido moiety at the anti-*T. cruzi* activity, 26 new compounds were tested *in vitro* against the *T. cruzi* parasite epimastigote and trypomastigote forms. Ultrastructural studies and flow cytometry analysis were also investigated (Fig. 1).

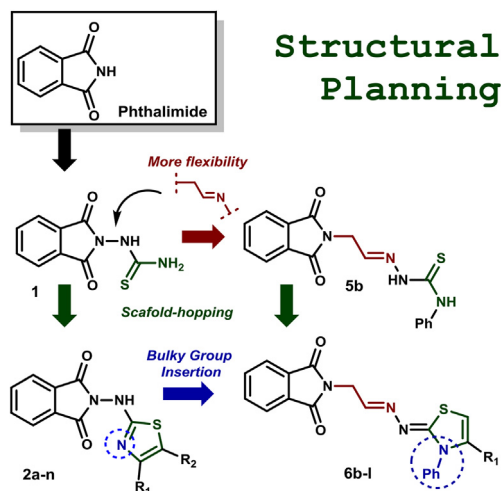


Fig. 1. Structural planning of the proposed compounds.

2. Results and discussion

2.1. Chemistry

Initially, 14 phthalimido-thiazoles (**2a-n**) were synthesized in a two-step reaction, following the procedures reported by Pessoa et al. [25]. Firstly, a reaction of phthalic anhydride with thiosemicarbazide, in DMF under reflux for 4 h, with a catalytic amount of DMAP, led us to compound **1**. The synthesis of the series **2a-n** was performed via Hantzsch cyclization between compound **1** and the appropriate α -halogenated ketone (1,3-dichloroacetone for compound **2a**), under ultrasound irradiation, at room temperature (rt) for 1 h. This reaction condition led to average yields from 36 to 65%. To synthesize the series **6a-l**, was followed the reaction protocol reported by Cardoso et al. [23]. The desired compounds **6a-l** were obtained by the reaction of Intermediate **5b** (or **5a**, for compound **6a**) with the appropriate α -halogenated ketone (1,3-dichloroacetone for compound **6a**), via Hantzsch cyclization, leading good yields (46–82%) (Scheme 1). All the synthesized compounds were well characterized by infrared (IR), nuclear magnetic resonance (^1H , ^{13}C NMR), mass spectroscopy (ESI-TOF) and, in case of compounds **2e**, **2f** and **2g**, by single crystal X-ray diffraction analysis (Fig. 2).

The ^1H NMR spectra of some compounds showed that phthalimido-thiazoles **6a-l** are composed by diastereomers. Next, we aimed to define the configuration of the major isomer by crystallographic analysis. However, we did not succeed in crystallizing phthalimido-thiazoles **6a-l** suitable for X-ray analysis. Based on previous crystallized compounds by our group, we suggest that the major isomer formed present the *E-Z* configuration (Fig. 3). Indeed, hydrazine double-bond $\text{C}2=\text{N}2$ is commonly assigned as *E* configuration [4,23,28]. Concerning the exocyclic double-bond $\text{N}3=\text{C}3$, we suggest that the predominant configuration is in *Z*-configuration [7,29]. Besides, a representative ^1H -NMR spectrum of compound **6i** is presented in Supplementary Material.

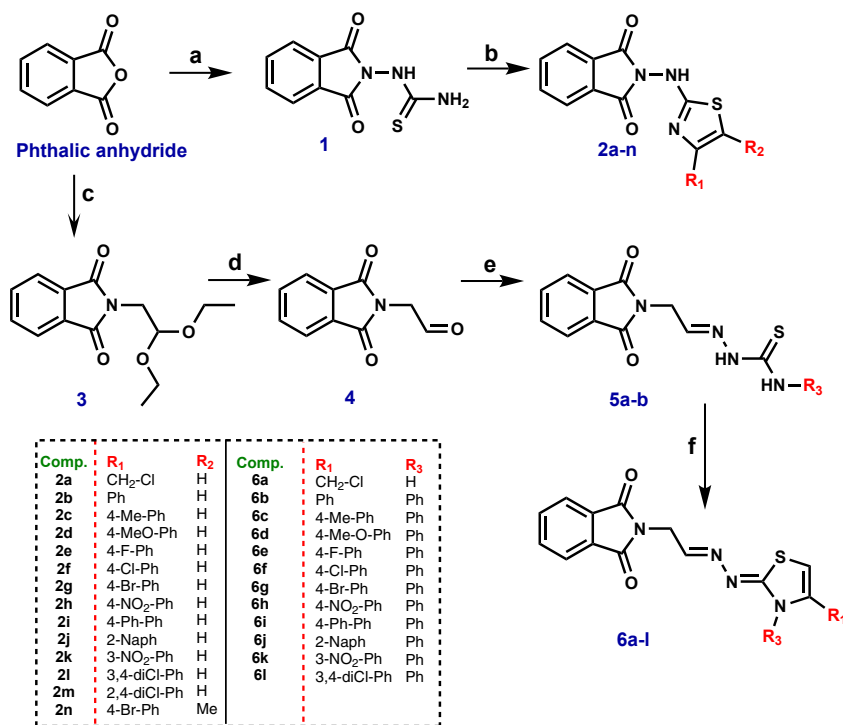
2.2. Anti-*T. cruzi* evaluation

Initially, compounds **2a-n** were planned to improve the trypanocidal activity and cytotoxic tolerance with the cyclization of phthalimido-thiosemicarbazone to the phthalimido-thiazole ring. From the results, it was observed in most of the cases that new phthalimido-thiazoles showed high cytotoxic activity in spleen cells. In opposition, only compounds **2i** and **2j** showed low cytotoxicity.

Concerning trypanocidal activity for epimastigotes, it is observed that 16 compounds (of 28) present better potency than Benznidazole (Table 1). Among series **2a-n**, compound **2i** was the most active, among the series and the entire work. The most active compound in series **6** is **6k**, a 3- NO_2 derivative, presenting an IC_{50} of 6.0 μM . Observing compounds with withdrawer substituents (**2e-h**, **2k-n**), compound 2,4-dichloro substituted (**2m**) was the most active. Its analogue disubstituted 3,4-dichloro (**2l**) present lower trypanocidal activity and high toxicity for BALB/c mice spleen cells, denoting that the orientation of the substituents is important for the activity. Observing bulk substituted compounds (phenyl, 2-naphthyl and 4-biphenyl), in series **2a-n**, a relationship of LogP and trypanocidal activity (Fig. 4) is observed, being compound **2i** the most active of this sub-series.

The trend of bulky substituents (LogP) observed for series **2a-n** is not observed for series **6a-l**, being compound **6k** (3- NO_2) the most active of the series **6a-l**.

When comparing the trypanocidal activity against the trypomastigote form of the series **2a-n** of phthalimido-thiazole derivatives, compound **2j** was found to be the most potent of this sub-



Scheme 1. Global synthesis of compounds **2a-n** and **6a-l**. Reagents and conditions: (a) thiosemicarbazide, DMF, DMAP, reflux, 4h; (b) corresponding α -halogenated ketone (1,3-dichloroacetone for compound **2a**), 2-propanol, ultrasound, rt, 1 h; (c) 1-aminoacetaldehyde diethyl acetal, toluene, reflux, DMAP, 2 h; (d) H₂SO₄ (70%), reflux, 2 h; (e) thiosemicarbazide (**5a**) or 4-phenyl-3-thiosemicarbazide (**5b**), EtOH, HCl, reflux, 4 h; (f) for **6a**, 1,3-dichloroacetone, DMF, rt, 1 h; for **6b-l**, corresponding α -halogenated ketone, 2-propanol, rt, 1 h.

series, presenting lower cytotoxic levels (269.2 μ M) and equipotent trypanocidal activity compared with BdZ (4.7 vs 6.3 μ M) (Table 1).

No clear correlation was observed between the substituents at the thiazole C4 and the biological activity. For example, 2-naphthyl is a bulky substituent present in **2j**; however, compound **2i**, which was also substituted with a bulky biphenyl substituent, did not present good activity. The influence of the phenyl linked at C4 in the thiazole ring was also investigated, but no noticeable improvement in activity was observed. Comparing compound **2a** with the phenyl-unsubstituted compound **2b**, a decrease in trypanocidal activity and higher cytotoxicity were observed, while the phenyl-substituted compounds maintained or increased both activities.

A structural optimization involving addition of a spacer group ($-\text{CH}_2-\text{CH}=\text{}$) between the phthalimide and the thiazole core was performed in order to increase the flexibility of the molecules and to investigate its influence on biological activities (Fig. 5). A substitution of H with phenyl at N3 was also performed to explore the influence of bulky substituents based on the results of compounds **2i** and **2j**, both substituted with 4-biphenyl and 2-naphthyl at C4, respectively, which displayed lower cytotoxicity.

Compounds that contained a spacer group (**6a-l**) and phenyl at N3 (**6b-l**) in general showed low cytotoxicity profiles and improved trypanocidal activity for trypanomastigote form, highlighting compounds **6a** (2.2 μ M), **6h** (3.2 μ M), **6j** (0.5 μ M) and **6k** (0.9 μ M). In fact, compound **6j** presented a selective index (SI, for trypanomastigote form) of 409.8, which was approximately 27-fold more selective than BdZ (SI: 15.25), the standard drug in clinical use. As observed in the **2a-n** series, the compound substituted at C4 with chloromethyl (**6a**, 2.2 μ M) was more active than compounds substituted with phenyl (**6b**, 8.8 μ M); indeed, phenyl-substituted compounds **6j** (0.5 μ M) and **6k** (0.9 μ M) were more active than **6a**. Comparing compound **6a** with **2a**, which were both substituted

with chloromethyl at C4 with the unique difference of the presence of the spacer group in **6a**, a 24-fold improvement in trypanocidal activity (2.2 vs 54.4 μ M) and a 4-fold increase in cytotoxicity (73.7 vs 17.0 μ M) were observed for **6a**. Compounds **6k** and **6h**, both nitro-substituted compounds at the *meta* and *para* positions, respectively, presented high trypanocidal activity with selective indexes of 114.9 and 64.6, respectively (Table 1). Compound **6e** (with the electron withdrawing fluorine substituent) and **6i** (with 4-biphenyl substituent) did not present good trypanocidal activity. Compound **6j**, which was substituted with the bulky substituent 2-naphthyl, presented the highest trypanocidal activity.

The SAR studies revealed that a series of phthalimido-thiazoles were interesting anti-*T. cruzi* compounds, which five new compounds showed low cytotoxicity in spleen cells of BALB/c mice and anti-trypanocidal activity against the trypomastigote form of the parasite.

Congreve et al. proposed a rule-of-three (RO3) [30] representing a set of guidelines for constructing a fragment library (molecular weight, <300; cLogP, ≤ 3 ; number of hydrogen bond donors, ≤ 3 ; and the number of hydrogen bond acceptors, ≤ 3). Recently, RO3 was accredited by most medicinal chemists and could be useful for efficient fragment selection [31]. As seen in Table 2, the phthalimide and thiazole fragments are in agreement with RO3.

The trypanocidal profile of these phthalimido-thiazoles revealed a group of privileged structure-based compounds that can be used as building blocks to obtain new lead-like compounds. They possess some structural features, such as lower molecular weights, decreased complexity and decreased hydrophobicity, which are consistent with lead-like characteristics. These compounds can be used to produce structurally simple leads with modest activity, allowing for further derivatization at a later stage to improve affinity and selectivity while retaining drug-like

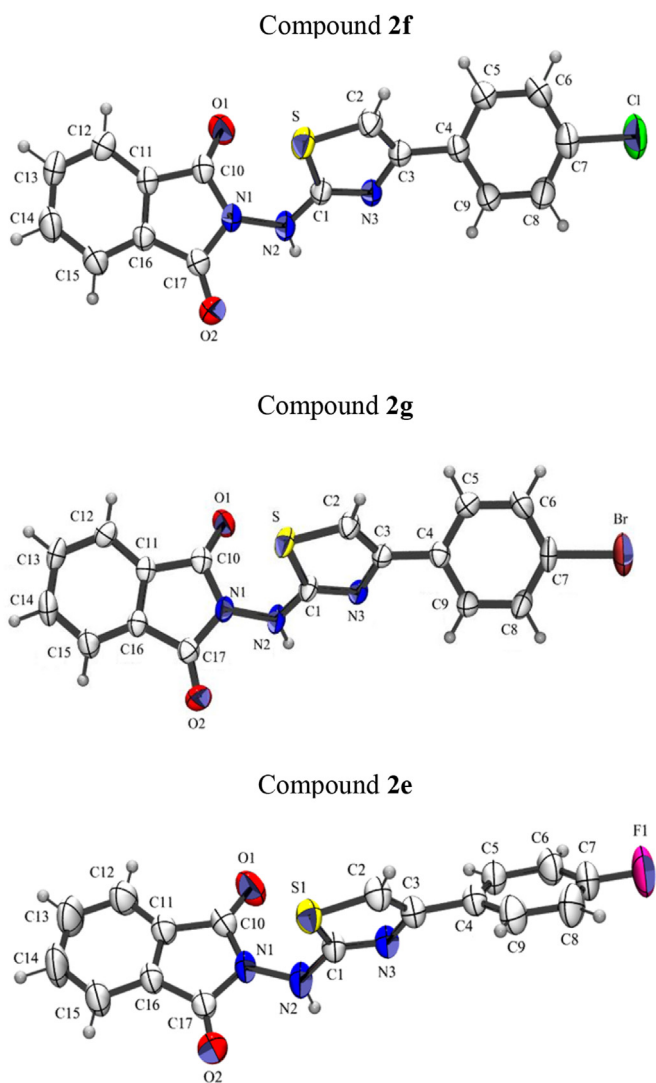


Fig. 2. The molecular structure of the title compounds showing the atom-labelling scheme and displacement ellipsoids at the 50% probability level.

characteristics.

2.3. Ultra structural studies

In view to investigate the effects of phthalimido-thiazoles on parasite morphology, compound **6k**, one of the most active compound of this work, was selected. The ultrastructural effects of **6k** on trypomastigotes after 24 h were analysed by TEM and SEM at the IC_{50} concentration and twice the IC_{50} value (Table 1), and the ultrastructural analysis showed several morphological alterations (Fig. 6).

SEM analysis revealed that treatment with 0.9 μM ($1 \times IC_{50}$) and 1.8 μM ($2 \times IC_{50}$) of **6k** caused blebs in the flagellum and shortening of the flagellum with a drastic decrease in the number of parasites, respectively (Fig. 6B–C), while the control group retained its typical morphology (Fig. 6A).

TEM analysis revealed that untreated parasites showed normal ultrastructural morphologies of organelles, such as kinetoplast, nucleus, nucleolus, flagellum, ribosomes and microtubule membranes (Fig. 6D), whereas parasites treated with 0.9 μM of **6k** showed alterations in the reservosomes, and a large number of cells showed intense cytoplasmic vacuolization. In addition, alterations

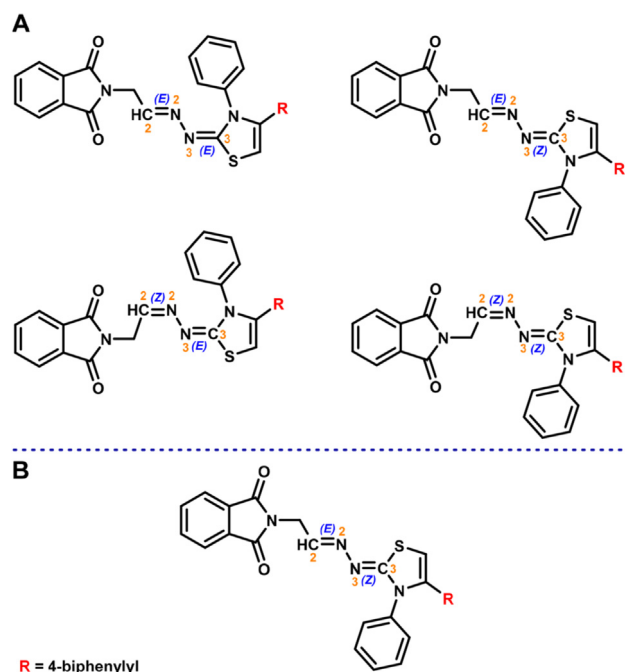


Fig. 3. Isomers representation of compound 6i. A- Possible isomers for compound 6i. B- Suggested isomer for compound 6i.

of the parasite morphology, large nuclear chromatin clumps that resembled the nuclei of apoptotic cells, mitochondria swelling and loss of cytoplasmic material were observed (Fig. 6E–F). The parasites treated with 1.8 μM of **6k** showed alterations of parasite morphology, abnormal chromatin condensation, dilated endoplasmic reticula, intense vacuolization in the cytoplasm, swelling of the kinetoplast and alterations in the reservosomes (Fig. 6G).

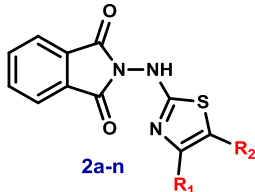
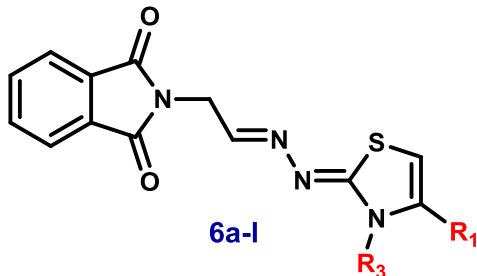
Ultrastructural analysis was applied to explore the damages induced by the drugs in trypomastigotes *T. cruzi* parasites and clearly showed severe morphological changes, of which intense cytoplasmic vacuolization, chromatin condensation, alterations in the reservosomes and swelling of the mitochondria were most frequent. These ultrastructural alterations are similar to those previously reported [32–36]. The ultrastructural evaluation indicated a dose-dependent action because a drastic decrease in the number of parasites was observed with increasing drug doses.

2.4. Flow cytometry analysis

After confirming that **6k** was an antiparasitic compound that affected ultrastructural cellular organization, we sought to determine whether **6k** caused parasite cell death. To this end, Y strain trypomastigotes were treated with different concentrations of **6k**. After 24 h incubation, parasite cells were stained with propidium iodide (PI) and annexin-V and analysed by flow cytometry. The results are shown in Fig. 7.

Compared with untreated cells, benzimidazole resulted in PI-staining in a concentration-dependent manner, while no significant annexin-V staining was observed (data not shown). At 25 μM , benzimidazole induced $56 \pm 6\%$ PI-staining in parasite cells. At the same concentration, treatment with compound **6k** induced PI-staining in $11 \pm 3\%$ of parasite cells. No PI or annexin-V staining were observed under treatment with **6k** (data not shown). Therefore, these phthalimido-thiazoles do not destroy parasite cells by classical cell death processes. Based on electronic microscopy observations, it is possible that phthalimido-thiazoles decrease

Table 1
Cytotoxicity and trypanocidal activity against epimastigotes and trypomastigotes forms.

CODE	R ₁	R ₂	R ₃	Cytotoxicity μM^{a}	IC ₅₀ epimastigotes (<i>T. cruzi</i>) - μM^{b}	IC ₅₀ trypomastigotes (<i>T. cruzi</i>) - μM^{c}
1	–	H	–	4.5	56.8	52.0
 2a-n						
2a	Cl–Me	H	–	17.0	225.7	54.4
2b	Ph	H	–	3.1	70.2	107.5
2c	4-Me-Ph	H	–	14.9	70.4	107.0
2d	4-Me-O-Ph	H	–	14.2	6.4	50.3
2e	4-F-Ph	H	–	2.9	26.5	52.1
2f	4-Cl-Ph	H	–	2.8	30.6	86.2
2g	4-Br-Ph	H	–	2.5	14.8	89.8
2h	4-NO ₂ -Ph	H	–	2.7	13.3	84.9
2i	4-Ph-Ph	H	–	251.6	4.0	27.5
2j	2-Naph	H	–	269.2	8.0	4.7
2k	3-NO ₂ -Ph	H	–	2.7	43.2	91.1
2l	3,4-diCl-Ph	H	–	2.6	69.3	88.8
2m	2,4-diCl-Ph	H	–	12.8	10.1	22.7
2n	4-Br-Ph	Me	–	2.4	13.9	38.2
5b	–	–	Ph	50	36.9	ND
 6a-l						
6a	Cl–Me	–	H	73.7	85.7	2.2
6b	Ph	–	Ph	228.1	ND	8.8
6c	4-Me-Ph	–	Ph	221.2	57.8	33.3
6d	4-Me-O-Ph	–	Ph	213.4	ND	10.0
6e	4-F-Ph	–	Ph	219.1	ND	73.8
6f	4-Cl-Ph	–	Ph	211.4	10.6	18.4
6g	4-Br-Ph	–	Ph	96.6	ND	9.7
6h	4-NO ₂ -Ph	–	Ph	206.8	12.2	3.2
6i	4-Ph-Ph	–	Ph	194.3	44.2	98.0
6j	2-Naph	–	Ph	204.9	11.9	0.5
6k	3-NO ₂ -Ph	–	Ph	103.4	6.0	0.9
6l	3,4-diCl-Ph	–	Ph	197.1	ND	ND
Bdz	–	–	–	96.1	48.8	6.3

^a Highest non-toxic concentration (>90% incorporation of tritiated thymidine) in spleen cells of BALB/c mice.

^b Determined 24 h after incubation of Y strain trypomastigotes with the compounds.

^c Determined 11 days after incubation of epimastigotes with the compounds.^{a,b} Only values with a standard deviation < 10% were included.^{a,b} IC₅₀ was calculated from at least five concentrations, in triplicate (SD < 10%). Bdz = Benznidazole; ND = Not Determined.

parasite viability by altering cytosol organization, mainly by causing intense cytoplasmic vacuolization.

3. Conclusion

Twenty-six phthalimido-thiazoles were obtained in reasonable yields using a simple methodology. Compounds with important trypanocidal activity, especially compounds **2j**, **6a**, **6h**, **6j** and **6k**, were identified. Flow cytometry and ultrastructural studies showed that compound **6k** did not kill the parasite via necrosis or apoptosis; however, it promoted several morphological changes in the parasite. Compound **6j**, the most potent trypanocidal agent identified in this work, presented a selective index of 409, which was approximately 26-fold more selective than Bdz, the standard

drug in clinical use. Our results indicated that phthalimido-thiazoles can be used as building blocks to design promising candidates to treat Chagas disease.

4. Experimental section

4.1. Chemistry

4.1.1. Equipment and reagents

All reagents were used as purchased from commercial sources (Sigma–Aldrich, Acros Organics, Vetec or Fluka). Reaction progress was followed by thin-layer chromatography (TLC) analysis (Merck, silica gel 60 F₂₅₄ in aluminium foil). The purities of the target compounds were confirmed by combustion analysis (for C, H, N,

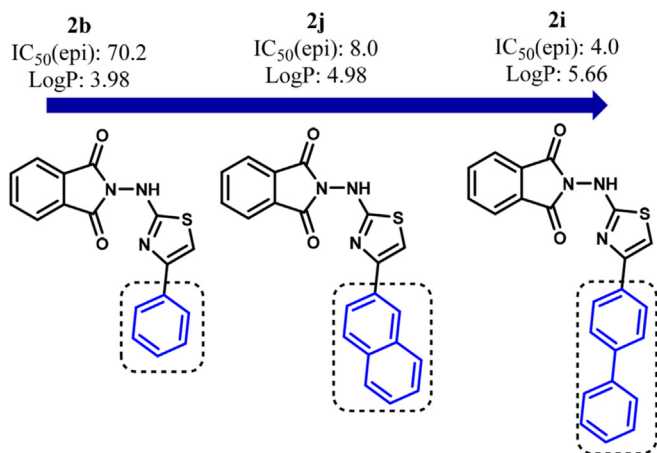


Fig. 4. Trend in trypanocidal activity for epimastigote form.

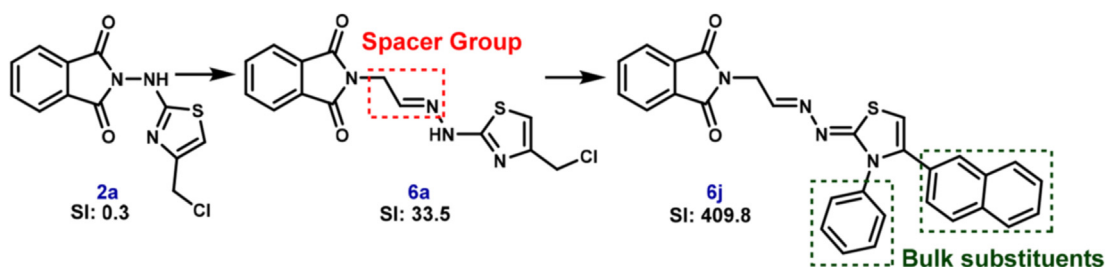


Fig. 5. Structural optimization of proposed compounds. Selective index (SI) = highest non-toxic concentration in spleen cells of BALB/c mice/IC₅₀ trypomastigotes.

Table 2

Rule-of-three (RO3) calculations of the fragments phthalimide and thiazole.

Rule	Phthalimide	Thiazole	Criteria met
Molecular weight (<300)	147.13	85.12	Yes
cLogP (<3)	1.148	0.486	Yes
Number of hydrogen bond donors (<3)	1	0	Yes
Number of hydrogen bond acceptors (<3)	2	1	Yes

and S) performed using a Carlo-Erba instrument (model EA 1110). Melting points were determined on a Fisatom 430D electrothermal capillary melting point apparatus and were uncorrected. NMR spectra were measured on either a Varian UnityPlus 400 MHz (400 MHz for ¹H and 100 MHz for ¹³C) or a Bruker AMX-300 MHz (300 MHz for ¹H and 75.5 MHz for ¹³C) instrument. DMSO-*d*₆ and D₂O were purchased from CIL or Sigma–Aldrich. Chemical shifts were reported in ppm, and multiplicities were given as s (singlet), d (doublet), t (triplet), m (multiplet), dd (double doublet), and coupling constants (*J*) in hertz. Mass spectrometry experiments were performed on a LC-IT-TOF (Shimadzu). Unless otherwise specified, ESI was conducted in positive ion mode. Typical conditions were as follows: capillary voltage of 3 kV, cone voltage of 30 V, and peak scan between 50 and 1000 *m/z*. IR spectra were recorded with a Bruker model IFS66 FT-IR spectrophotometer using KBr pellets.

4.1.2. General procedure for the syntheses of 2a–n

The compound **1** was prepared by reacting commercially available thiosemicarbazide with the phthalic anhydride (1:1 mol ratio) using DMF under reflux in the presence of a catalytic amount of DMAP, for 4 h. This reaction condition led to satisfactory yield (58%). The phthalimido-thiazoles (**2a–n**) were prepared via

cyclization between **1** and respective α -halogenated ketone (1,3-dichloroacetone for compound **2a**), via ultrasound irradiation for 1 h, as previously related [4]. These reactions proceeded well under ultrasound conditions at room temperature using 2-propanol as solvent, resulting in satisfactory yields (36–65%) and shorter reaction times (60 min in most cases).

4.1.2.1. 2-[4-(chloromethyl)thiazol-2-ylamino]isoindoline-1,3-dione (**2a**). White crystals; Yield: 50%; m.p. (°C) 207–208; Rf: 0.53 (hexane/ethyl acetate 1:1). IR (KBr, cm⁻¹): 3119.15 (NH), 1743.24 (C=O). ¹H NMR (300 MHz, DMSO-*d*₆), δ ppm: 4.54 (s, 2H, CH₂), 7.03 (s, 1H, thiazole), 7.93–7.99 (m, 4H, Ar), 10.54 (s, 1H, NH). ¹³C NMR (75.5 MHz, DMSO-*d*₆), δ ppm: 41.1 (CH₂), 109.8 (CH, thiazole), 123.9 (CH, Ar), 129.4 (C, Ar), 135.4 (CH, Ar), 147.1 (C, thiazole), 165.6 (C=O), 168.3 (S–C=N, thiazole). Anal. Calcd for C₁₂H₈ClN₃O₂S: C, 49.07; H, 2.75; N, 14.31; S, 10.92. found: C, 48.50; H, 2.81; N, 14.34; S 10.43. HRMS: 294.0097 [M+H]⁺.

4.1.2.2. 2-(4-Phenylthiazol-2-ylamino)isoindoline-1,3-dione (**2b**). Light yellow crystals; Yield: 65%; m.p. (°C) 194–196; Rf: 0.60 (hexane/ethyl acetate 1:1). IR (KBr, cm⁻¹): 3123.66 (NH), 1742.23 (C=O). ¹H NMR (400 MHz, DMSO-*d*₆), δ ppm: 7.25 (t, *J* = 7.4 Hz, 1H, Ar), 7.33 (t, *J* = 7.4 Hz, 2H, Ar), 7.38 (s, 1H, thiazole), 7.70 (d, *J* = 7.6 Hz, 2H, Ar), 7.95–8.02 (m, 4H, Ar), 10.65 (s, 1H, NH). ¹³C NMR (100 MHz, DMSO-*d*₆), δ ppm: 104.8 (CH, thiazole), 123.8 (CH, Ar), 125.5 (CH, Ar), 127.7 (CH, Ar), 128.6 (CH, Ar), 129.3 (C, Ar), 133.9 (C, Ar), 135.4 (CH, Ar), 149.9 (C, thiazole), 165.5 (C=O), 167.6 (S–C=N, thiazole). Anal. Calcd for C₁₇H₁₁N₃O₂S: C, 62.08; H, 3.41; N, 12.98; S, 9.71. found: C, 63.54; H, 3.45; N, 12.53; S, 9.98. HRMS: 322.0619 [M+H]⁺.

4.1.2.3. 2-(4-*p*-Tolylthiazol-2-ylamino)isoindoline-1,3-dione (**2c**). Light yellow crystals; Yield: 37%; m.p. (°C) 214–216; Rf: 0.65 (hexane/ethyl acetate 1:1). IR (KBr, cm⁻¹): 3117.64 (NH), 1738.51 (C=O). ¹H NMR (400 MHz, DMSO-*d*₆), δ ppm: 2.26 (s, 3H, CH₃), 7.14 (d, *J* = 6.8 Hz, 2H, Ar), 7.30 (s, 1H, thiazole), 7.59 (d, *J* = 6.8 Hz, 2H, Ar), 7.99 (m, 4H, Ar), 10.41 (s, 1H, NH). ¹³C NMR (100 MHz, DMSO-*d*₆), δ ppm: 20.8 (CH₃), 103.9 (CH, thiazole), 123.9 (CH, Ar), 125.5 (CH, Ar), 129.17 (CH, Ar), 129.3 (C, Ar), 131.4 (C, Ar), 135.4 (C, Ar), 137.1 (C, Ar), 150.2 (C, thiazole), 165.6 (C=O), 167.5 (S–C=N, thiazole). Anal. Calcd for C₁₈H₁₃N₃O₂S: C, 63.17; H, 3.81; N, 18.12; S, 9.17. found: C,

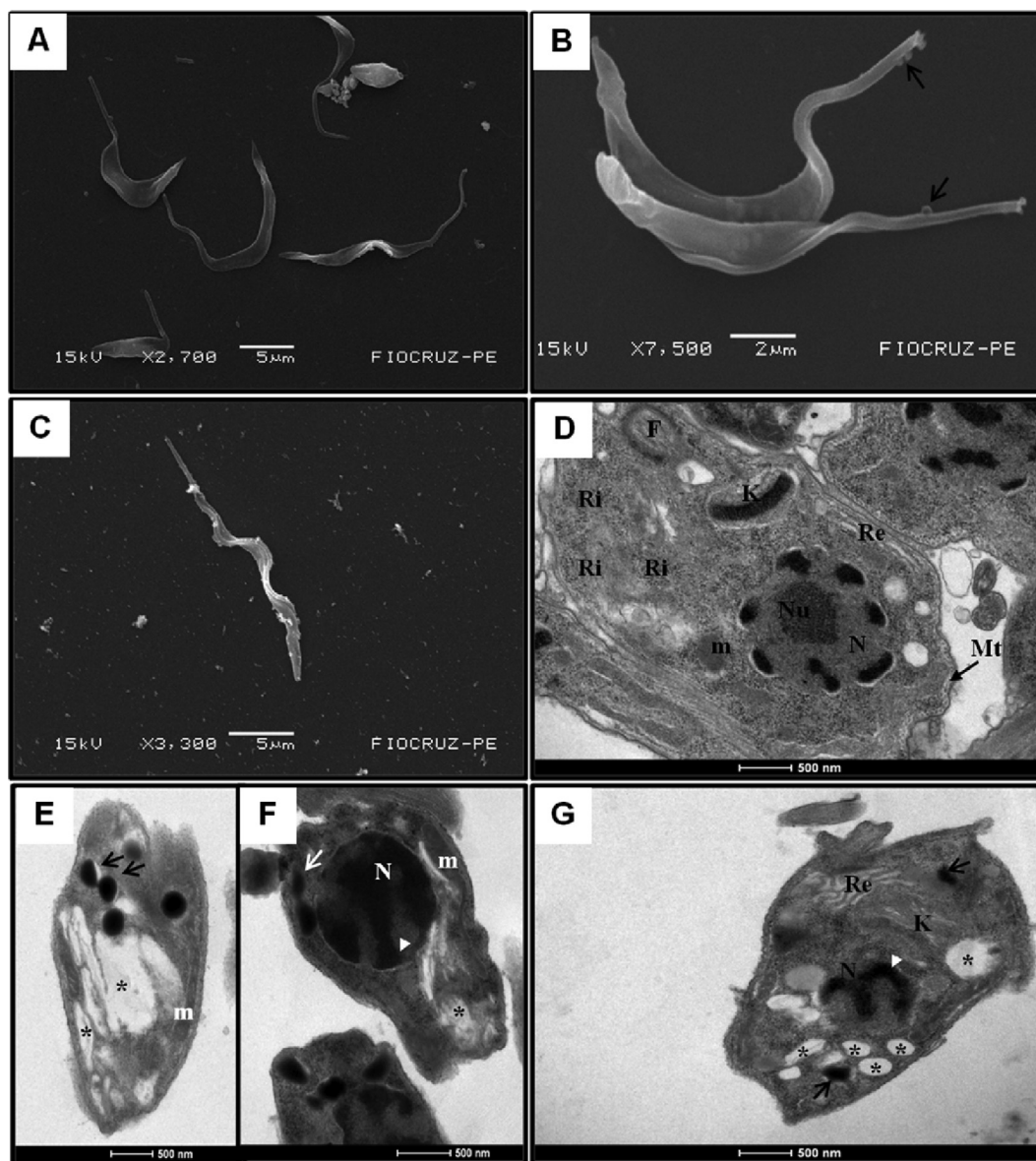


Fig. 6. Ultrastructural alterations in trypanostigotes forms of *T. cruzi* treated with 6k as observed by SEM and TEM. A- SEM of control untreated trypanostigotes showing the typical elongated body. B- SEM of parasite treated with 0.9 μM of 6k showing blebs in the flagellum. C- SEM of parasite treated with 1.8 μM of 6k showing drastic reduction in the number of parasites and shortening of the flagellum. D- TEM of untreated trypanostigotes showing the normal morphology with kinetoplast (K), nucleus (N), nucleolus (Nu), flagellum (F), ribosomes (Ri), mitochondria (m) and Microtubules (Mt). E and F- TEM of parasite treated with 0.9 μM of 6k showing alterations of the parasite morphology, abnormal chromatin condensation (arrowhead) no nucleus (N), swelling of the mitochondrion (m), alterations in the reservosomes (arrows) and loss of cytoplasmic material (asterisks). G- TEM of parasite treated with 1.8 μM of 6k showing alterations of the parasite morphology, abnormal chromatin condensation (arrowhead), endoplasmic reticulum dilated (Re), intense vacuolization in the cytoplasm (asterisk), swelling of the kinetoplast (K) and alterations in the reservosomes (arrows).

64.46; H, 3.91; N, 18.53; S, 9.56. HRMS: 336.0812 $[\text{M}+\text{H}]^+$.

4.1.2.4. 2-[4-(4-methoxyphenyl)thiazol-2-ylamino]isoindoline-1,3-dione (2d). Light yellow crystals; Yield: 72%; m.p. ($^{\circ}\text{C}$) 215–218; Rf: 0.53 (hexane/ethyl acetate 3:2). IR (KBr, cm^{-1}): 3232.68 (NH), 1748.64 (C=O). ^1H NMR (300 MHz, DMSO- d_6), δ ppm: 1.025 (s, 3H, CH₃), 6.90 (d, $J = 11.6$ Hz, 2H, Ar), 7.20 (s, 1H, thiazole), 7.62 (d, $J = 11.6$ Hz, 2H, Ar), 7.98 (m, 4H, Ar), 10.72 (s, 1H, NH). ^{13}C NMR (75.5 MHz, DMSO- d_6), δ ppm: 25.5 (CH₃), 102.7 (CH, thiazole), 114.0 (CH, Ar), 123.9 (CH, Ar), 126.7 (C, Ar), 127.0 (CH, Ar), 129.4 (C, Ar), 135.4 (CH, Ar), 149.5 (C, thiazole), 158.6 (CO, Ar), 165.6 (C=O), 167.6 (S=C=N, thiazole). Anal. Calcd for C₁₈H₁₃N₃O₃S: C, 58.88; H, 3.87; N, 11.38; S, 8.77. found: C, 61.53; H, 3.73; N, 11.96; S, 9.13. HRMS: 352.0825 $[\text{M}+\text{H}]^+$.

4.1.2.5. 2-[4-(4-fluorophenyl)thiazol-2-ylamino]isoindoline-1,3-dione (2e). Yellow crystals; Yield: 51%; m.p. ($^{\circ}\text{C}$) 208–210; Rf: 0.53 (hexane/ethyl acetate 3:2). IR (KBr, cm^{-1}): 3130.14 (NH), 1743.63 (C=O). ^1H NMR (400 MHz, DMSO- d_6), δ ppm: 7.17 (d, $J = 17.6$ Hz, 2H, Ar), 7.37 (s, 1H, thiazole), 7.73 (d, $J = 14.0$ Hz, 2H, Ar), 7.99 (m, 4H, Ar), 10.42 (s, 1H, NH). ^{13}C NMR (100 MHz, DMSO- d_6), δ ppm: 104.6 (CH, thiazole), 115.4 (CH, Ar), 115.6 (CH, Ar), 123.9 (CH, Ar), 127.5 (CH, Ar), 129.3 (C, Ar), 135.4 (CH, Ar), 160.4 (C, thiazole), 162.9 (CF, Ar), 165.5 (C=O), 167.6 (S=C=N, thiazole). Anal. Calcd for C₁₇H₁₀FN₃O₂S: C, 60.32; H, 3.02; N, 12.32; S, 9.58. found: C, 60.17; H, 2.97; N, 12.38; S, 9.45. HRMS: 340.0566 $[\text{M}+\text{H}]^+$.

4.1.2.6. 2-[4-(4-chlorophenyl)thiazol-2-ylamino]isoindoline-1,3-dione (2f). Light yellow crystals; Yield: 62%; m.p. ($^{\circ}\text{C}$) 217–218; Rf:

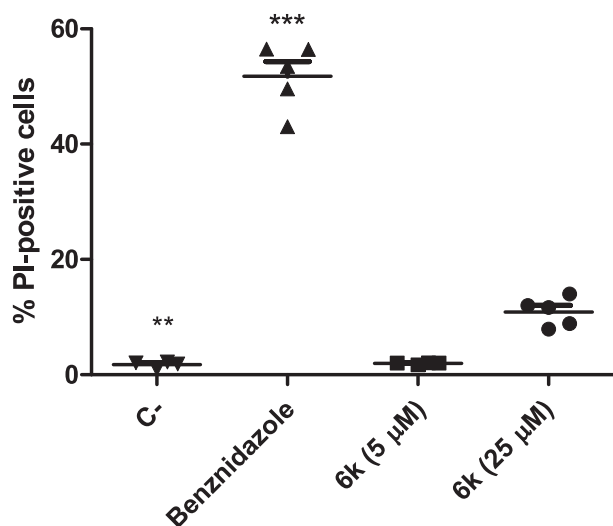


Fig. 7. % of PI-positive cells analysis under 6k treatment. Trypomastigotes were treated with complex for 24 h and examined by flow cytometry with PI staining. (C-) Untreated; Drug concentration is given in parenthesis. Two independent experiments, each concentration in duplicate. *** $p < 0.0001$ in comparison to (C-).

0.53 (hexane/ethyl acetate 1:1). IR (KBr, cm^{-1}): 3119.79 (NH), 1739.00 (C=O). $^1\text{H NMR}$ (400 MHz, $\text{DMSO-}d_6$), δ ppm: 7.39 (d, $J = 8.0$ Hz, 2H, Ar), 7.46 (s, 1H, thiazole), 7.72 (d, $J = 8$ Hz, 2H, Ar), 7.99 (m, 4H, Ar), 10.46 (s, 1H, NH). $^{13}\text{C NMR}$ (100 MHz, $\text{DMSO-}d_6$), δ ppm: 105.7 (CH, thiazole), 123.9 (CH, Ar), 127.3 (CH, Ar), 128.7 (CH, Ar), 129.3 (C, Ar) 132.2 (C, Ar), 132.9 (C, Ar), 135.4 (C, Ar), 148.9 (C, thiazole), 165.5 (C=O), 167.7 (S–C=N, thiazole). Anal. Calcd for $\text{C}_{17}\text{H}_{10}\text{ClN}_3\text{O}_2\text{S}$: C, 57.55; H, 2.96; N, 11.62; S, 9.03. found: C, 57.39; H, 2.83; N, 11.81; S, 9.01. HRMS: 356.0260 $[\text{M}+\text{H}]^+$.

4.1.2.7. 2-[4-(4-bromophenyl)thiazol-2-ylamino]isoindoline-1,3-dione (**2g**). Light yellow crystals; Yield: 55%; m.p. ($^\circ\text{C}$) 220–221; Rf: 0.68 (hexane/ethyl acetate 1:1). IR (KBr, cm^{-1}): 3117.68 (NH), 1739.19 (C=O). $^1\text{H NMR}$ (400 MHz, $\text{DMSO-}d_6$), δ ppm: 7.47 (s, 1H, thiazole), 7.53 (d, $J = 8.4$ Hz, 2H, Ar), 7.65 (d, $J = 8.0$ Hz, 2H, Ar), 7.96 (m, 4H, Ar), 10.46 (s, 1H, NH). $^{13}\text{C NMR}$ (100 MHz, $\text{DMSO-}d_6$), δ ppm: 105.8 (CH, thiazole), 120.8 (CH, Ar), 123.9 (CH, Ar), 127.6 (CH, Ar), 129.3 (C, Ar) 131.6 (C, Ar), 135.4 (C, Ar), 148.9 (C, thiazole), 165.5 (C=O), 167.7 (S–C=N, thiazole). Anal. Calcd for $\text{C}_{17}\text{H}_{10}\text{BrN}_3\text{O}_2\text{S}$: C, 51.15; H, 2.58; N, 11.62; S, 9.03. found: C, 51.01; H, 2.52; N, 11.50; S, 8.91. HRMS: 401.9764 $[\text{M}+\text{H}]^+$.

4.1.2.8. 2-[4-(4-nitrophenyl)thiazol-2-ylamino]isoindoline-1,3-dione (**2h**). Yellow crystals; Yield: 41%; m.p. ($^\circ\text{C}$) 239–240; Rf: 0.45 (hexane/ethyl acetate 3:2). IR (KBr, cm^{-1}): 3309.85 (NH), 1724.82 (C=O). $^1\text{H NMR}$ (400 MHz, $\text{DMSO-}d_6$), δ ppm: 7.77 (s, 1H, thiazole), 7.97 (m, 4H, Ar), 8.02 (d, $J = 8.8$ Hz, 2H, Ar), 8.21 (d, $J = 8.8$ Hz, 2H, Ar), 10.54 (s, 1H, NH). $^{13}\text{C NMR}$ (100 MHz, $\text{DMSO-}d_6$), δ ppm: 109.6 (CH, thiazole), 123.9 (CH, Ar), 124.1 (CH, Ar), 126.4 (CH, Ar), 129.3 (CN Ar), 135.4 (CH, Ar), 139.9 (C, Ar), 146.3 (C, Ar), 147.9 (C, thiazole), 165.382 (C=O), 168.0 (S–C=N, thiazole). Anal. Calcd for $\text{C}_{17}\text{H}_{10}\text{N}_4\text{O}_4\text{S}$: C, 54.40; H, 2.87; N, 15.23; S, 9.11. found: C, 55.73; H, 2.75; N, 15.29; S, 8.75. HRMS: 367.0517 $[\text{M}+\text{H}]^+$.

4.1.2.9. 2-[4-(biphenyl-4-yl)thiazol-2-ylamino]isoindoline-1,3-dione (**2i**). Light yellow crystals; Yield: 46%; m.p. ($^\circ\text{C}$) 240–241; Rf: 0.65 (hexane/ethyl acetate 3:2). IR (KBr, cm^{-1}): 3324.67 (NH), 1660.10 (C=O). $^1\text{H NMR}$ (300 MHz, $\text{DMSO-}d_6$), δ ppm: 7.35 (s, 1H, thiazole), 7.48 (t, $J = 10.0$ Hz, 1H, Ar), 7.63 (m, 4H, Ar), 7.72 (d, $J = 11.6$ Hz, 2H, Ar), 7.82 (m, 4H, Ar) 7.96 (d, $J = 11.6$ Hz, 2H, Ar), 10.65 (s, 1H, NH). ^{13}C

NMR (75.5 MHz, $\text{DMSO-}d_6$), δ ppm: 103.4 (CH, thiazole), 126.5 (CH, Ar), 126.9 (CH, Ar), 127.5 (CH, Ar), 128.0 (CH, Ar) 129.0 (CH, Ar), 130.1 (CH, Ar), 131.5 (CH, Ar), 133.9 (C, Ar), 136.1 (CH, Ar), 139.0 (C, Ar), 139.7 (C, Ar), 150.2 (C, thiazole), 167.6 (C=O), 168.3 (S–C=N, thiazole). Anal. Calcd for $\text{C}_{23}\text{H}_{15}\text{N}_3\text{O}_2\text{S}$: C, 66.81; H, 3.98; N, 10.48; S, 7.95. found: C, 66.50; H, 3.80; N, 10.57; S, 8.07. HRMS: 398.0958 $[\text{M}+\text{H}]^+$.

4.1.2.10. 2-[4-(naphthalen-2-yl)thiazol-2-ylamino]isoindoline-1,3-dione (**2j**). Light yellow crystals; Yield: 47%; m.p. ($^\circ\text{C}$) 225–227; Rf: 0.50 (hexane/ethyl acetate 3:2). IR (KBr, cm^{-1}): 3169.87 (NH), 1743.89 (C=O). $^1\text{H NMR}$ (400 MHz, $\text{DMSO-}d_6$), δ ppm: 7.47 (t, 2H, Ar), 7.53 (s, 1H, thiazole), 7.87 (d, $J = 11.6$ Hz, 4H, Ar), 8.03 (m, 4H, Ar), 8.23 (s, 1H, Ar), 10.48 (s, 1H, NH). $^{13}\text{C NMR}$ (100 MHz, $\text{DMSO-}d_6$), δ ppm: 105.5 (CH, thiazole), 123.9 (CH, Ar), 124.2 (CH, Ar), 126.1 (CH, Ar), 126.4 (CH, Ar) 127.1 (CH, Ar), 127.6 (CH, Ar), 128.1 (CH, Ar), 128.2 (CH, Ar), 129.3 (C, Ar), 131.5 (C, Ar), 132.4 (C, Ar), 133.0 (C, Ar), 135.4 (CH, Ar), 150.1 (C, thiazole), 165.6 (C=O), 168.0 (S–C=N, thiazole). Anal. Calcd for $\text{C}_{21}\text{H}_{13}\text{N}_3\text{O}_2\text{S}$: C, 64.89; H, 3.48; N, 11.45; S, 8.26. found: C, 67.91; H, 3.53; N, 11.11; S, 8.63. HRMS: 367.0517 $[\text{M}+\text{H}]^+$.

4.1.2.11. 2-[4-(3-nitrophenyl)thiazol-2-ylamino]isoindoline-1,3-dione (**2k**). Light yellow crystals; Yield: 44%; m.p. ($^\circ\text{C}$) 206–207; Rf: 0.55 (hexane/ethyl acetate 3:2). IR (KBr, cm^{-1}): 3287.35 (NH), 1732.47 (C=O). $^1\text{H NMR}$ (300 MHz, $\text{DMSO-}d_6$), δ ppm: 7.65 (t, $J = 7.2$ Hz, 1H, Ar), 7.73 (s, 1H, thiazole), 8.00 (m, 4H, Ar), 8.13 (m, 2H, Ar), 8.48 (s, 1H, Ar) 10.36 (s, 1H, NH). $^{13}\text{C NMR}$ (75.5 MHz, $\text{DMSO-}d_6$), δ ppm: 107.7 (CH, thiazole), 119.9 (CH, Ar), 122.3 (CH, Ar), 123.9 (CH, Ar), 129.3 (CN, Ar) 130.3 (CH, Ar), 131.7 (CH, Ar), 135.5 (CH, Ar), 147.7 (C, Ar), 148.2 (C, thiazole), 165.5 (C=O), 168.2 (S–C=N, thiazole). Anal. Calcd for $\text{C}_{17}\text{H}_{10}\text{N}_4\text{O}_4\text{S}$: C, 53.04; H, 2.88; N, 15.49; S, 8.90. found: C, 54.73; H, 2.75; N, 15.29; S, 8.75. HRMS: 367.0517 $[\text{M}+\text{H}]^+$.

4.1.2.12. 2-[4-(3,4-dichlorophenyl)thiazol-2-ylamino]isoindoline-1,3-dione (**2l**). Light yellow crystals; Yield: 57%; m.p. ($^\circ\text{C}$) 217–218; Rf: 0.53 (hexane/ethyl acetate 3:2). IR (KBr, cm^{-1}): 3337.03 (NH), 1742.53 (C=O). $^1\text{H NMR}$ (300 MHz, $\text{DMSO-}d_6$), δ ppm: 7.52 (s, 1H, thiazole), 7.62 (s, 1H, Ar), 7.68 (d, $J = 2.1$ Hz, 1H, Ar), 7.94 (d, $J = 1.8$ Hz, 1H, Ar), 8.00 (m, 4H, Ar), 10.51 (s, 1H, NH). $^{13}\text{C NMR}$ (75.5 MHz, $\text{DMSO-}d_6$), δ ppm: 107.1 (CH, thiazole), 123.9 (CH, Ar), 127.1 (CH, Ar), 129.3 (C, Ar), 129.5 (CH, Ar), 130.9 (C, Ar), 131.4 (C, Ar), 134.5 (CH, Ar), 135.4 (C, Ar), 136.0 (CH, Ar), 147.9 (C, thiazole), 165.4 (C=O), 167.9 (S–C=N, thiazole). Anal. Calcd for $\text{C}_{17}\text{H}_9\text{Cl}_2\text{N}_3\text{O}_2\text{S}$: C, 51.19; H, 2.43; N, 11.04; S, 8.58. found: C, 52.32; H, 2.32; N, 10.77; S, 8.22. HRMS: 356.0260 $[\text{M}+\text{H}]^+$.

4.1.2.13. 2-[4-(2,4-dichlorophenyl)thiazol-2-ylamino]isoindoline-1,3-dione (**2m**). Colourless crystals; Yield: 46%; m.p. ($^\circ\text{C}$) 217–218; Rf: 0.55 (hexane/ethyl acetate 3:2). IR (KBr, cm^{-1}): 3130.90 (NH), 1741.75 (C=O). $^1\text{H NMR}$ (400 MHz, $\text{DMSO-}d_6$), δ ppm: 7.41 (d, $J = 7.2$ Hz, 1H, Ar), 7.45 (s, 1H, thiazole), 7.63 (s, 1H, Ar), 7.65 (d, $J = 8.4$ Hz, 1H, Ar), 7.97 (m, 4H, Ar), 10.46 (s, 1H, NH). $^{13}\text{C NMR}$ (100 MHz, $\text{DMSO-}d_6$), δ ppm: 110.45 (CH, thiazole), 123.8 (CH, Ar), 127.5 (CH, Ar), 129.3 (C, Ar), 129.7 (CH, Ar), 131.5 (C, Ar), 131.5 (C, Ar), 132.1 (CH, Ar), 132.7 (C, Ar), 135.4 (CH, Ar), 145.4 (C, thiazole), 165.4 (C=O), 166.7 (S–C=N, thiazole). Anal. Calcd for $\text{C}_{17}\text{H}_9\text{Cl}_2\text{N}_3\text{O}_2\text{S}$: C, 52.25; H, 2.26; N, 10.50; S, 7.91. found: C, 52.32; H, 2.32; N, 10.77; S, 8.22. HRMS: 356.0260 $[\text{M}+\text{H}]^+$.

4.1.2.14. 2-[4-(4-bromophenyl)-5-methylthiazol-2-ylamino]isoindoline-1,3-dione (**2n**). Yellow crystals; Yield: 36%; m.p. ($^\circ\text{C}$) 235–236; Rf: 0.60 (hexane/ethyl acetate 3:2). IR (KBr, cm^{-1}): 3188.90 (NH), 1745.97 (C=O). $^1\text{H NMR}$ (400 MHz, $\text{DMSO-}d_6$), δ ppm: 2.36 (s, 3H, CH_3), 7.41 (d, $J = 8.4$ Hz, 2H, Ar), 7.55 (d, $J = 8.4$ Hz, 2H, Ar), 7.96 (m, 4H, Ar), 10.23 (s, 1H, NH); $^{13}\text{C NMR}$ (100 MHz, $\text{DMSO-}d_6$), δ ppm: 12.1

(CH₃), 119.3 (C, thiazole), 120.4 (C, Ar), 123.8 (CH, Ar), 129.3 (C, Ar), 129.8 (CH, Ar), 131.2 (CH, Ar), 133.7 (CBr, Ar), 135.3 (CH, Ar), 144.0 (C, thiazole), 163.5 (C=O), 165.5 (S–C=N, thiazole). Anal. Calcd for C₁₇H₁₂BrN₃O₂S: C, 51.75; H, 3.00; N, 9.93; S, 7.58. found: C, 52.19; H, 2.92; N, 10.10; S, 7.74. HRMS: 401.9764 [M+H]⁺.

4.1.3. Procedure for the syntheses of intermediate compounds 5a–b

Compound **3** was prepared by the condensation of commercially available aminoacetaldehyde diethyl acetal with the phthalic anhydride (1:1 mol ratio), using toluene under reflux, in the presence of a catalytic amount of DMAP (yield 52%) for 2 h. In the next step, 2-(2,2-diethoxyethyl)isoindoline-1,3-dione (**3**) underwent acid hydrolysis (sulphuric acid at 70%) in reflux for 2 h. After the reaction was completed, it was allowed to reach at room temperature and was then cooled to induce precipitation. The formed precipitate was filtered on a sintered funnel with distilled water, yielding 55% of the pure product. For the synthesis of **5a** and **5b**, 2-(1,3-dioxoisindol-2-yl) acetaldehyde (**4**) reacted with thiosemicarbazide (in the ratio 1:1) (for **5a**) or 4-phenyl-3-thiosemicarbazide (for **5b**), in ethanol, under reflux with catalytic amount of HCl (4 drops) for 4 h. The reactions were followed by thin layer chromatographic plate analysis. The formed precipitate was filtered on a sintered funnel with ethanol to yield the pure product (yield 76% for **5a** and 70% for **5b**).

4.1.3.1. (*E*)-2-[2-(1,3-dioxoisindolin-2-yl)ethylidene]hydrazinecarbothioamide (**5a**). White crystals; Yield: 76%; m.p. (°C) 223–224; Rf 0.45 (hexane/ethyl acetate 3:2); IR (KBr, cm⁻¹): 3423 and 3308 (N–H), 1769 and 1713 (C=O), 1602 (C=N); ¹H NMR (300 MHz, DMSO-*d*₆), δ ppm: 4.36 (d, *J* = 3.6 Hz, 2H, CH₂), 7.36 (s, 1H, NH), 7.42 (t, *J* = 3.6 Hz, 1H, CH=N), 7.83–7.90 (m, 4H, Ar), 8.03 and 11.27 (s, 1H, NH₂); ¹³C NMR (75.5 MHz, DMSO-*d*₆), δ ppm: 40.1 (CH₂), 123.1 (Ar), 131.7 (Ar), 134.4 (Ar), 140.4 (C=N), 167.5 (C=O), 177.9 (C=S). Anal. Calcd for C₁₁H₁₀N₄O₂S: C, 50.37; H, 3.84; N, 21.36; S, 12.22. found: C, 50.03; H, 3.45; N, 20.98; S, 12.30. HRMS: 262.3388 [M+H]⁺.

4.1.3.2. (*E*)-2-[2-(1,3-dioxoisindolin-2-yl)ethylidene]-*N*-phenylhydrazinecarbothioamide (**5b**). White crystals; Yield: 70%; m.p. (°C) 174–176; Rf 0.52 (hexane/ethyl acetate 3:2); ¹H NMR (300 MHz, DMSO-*d*₆), δ ppm: 4.46 (d, *J* = 4.2 Hz, 2H, CH₃), 7.14 (t, *J* = 7.8 Hz, 1H, Ar), 7.29 (t, *J* = 7.8 Hz, 2H, Ar), 7.42 (d, *J* = 7.8 Hz, 2H), 7.52 (t, *J* = 4.2 Hz, 1H, Ar), 7.85–7.99 (m, 4H, Ar), 9.66 (s, 1H, NH), 11.72 (s, 1H, NH); ¹³C NMR (75.5 MHz, DMSO-*d*₆), δ ppm: 40 (CH₂), 123.2 (Ar), 124.7 (Ar), 125.1 (Ar), 128.1 (Ar), 131.7 (Ar), 134.5 (Ar), 138.7 (Ar), 140.9 (C=N), 167.6 (C=O), 175.8 (C=S). Anal. Calcd for C₁₇H₁₄N₄O₂S: C, 60.34; H, 4.17; N, 16.56; S, 9.48. found: C, 60.03; H, 4.45; N, 16.35; S, 11.30. HRMS: 339.0845 [M+H]⁺.

4.1.4. Procedure for the synthesis of 6a

In a round bottom flask was added 2-(2-(1,3-dioxoisindolin-2-yl) ethylidene)hydrazinecarbothioamide (**5a**), 1,3-dichloroacetone and DMF. The reaction mixture was stirred at room temperature for about 1 h. The reaction was followed by thin layer chromatographic plate. After addition of distilled water, the pure product precipitates.

4.1.4.1. (*E*)-2-(2-[2-[4-(chloromethyl)thiazol-2-yl]hydrazono]ethyl)isoindoline-1,3-dione (**6a**). White crystals; Yield: 82%; m.p. (°C) 191–193; Rf 0.23 (hexane/ethyl acetate 3:2); IR (KBr, cm⁻¹): 3159.36 and 3113.44 (N–H), 1771.01 and 1717.67 (C=O), 1565.77 (C=N). ¹H NMR (400 MHz, DMSO-*d*₆), δ ppm: 4.41 (d, *J* = 3.2 Hz, 2H, CH₂), 4.53 (s, 2H, CH₂), 6.76 (s, 1H, CH, thiazole), 7.32 (s, 1H, CH), 7.86–7.89 (m, 4H, CH Ar), 11.75 (s, 1H, NH); ¹³C NMR (75.5 MHz, DMSO-*d*₆), δ ppm: 38 (CH₂), 41.7 (CH₂), 107.9 (CH, thiazole), 123.1

(Ar), 131.7 (Ar), 134.5 (Ar), 138.4 (C, thiazole), 147.8 (C=N), 167.5 (C=O), 168.6 (S–C=N, thiazole). Anal. Calcd for C₁₄H₁₁ClN₄O₂S: C, 50.23; H, 3.31; N, 16.74; S, 9.58. found: C, 49.91; H, 3.30; N, 16.82; S, 10.03. HRMS: 335.0463 [M+H]⁺.

4.1.5. General procedure for the synthesis of 6b–l

In round bottom flask was added 2-(2-(1,3-dioxoisindolin-2-yl)ethylidene)-*N*-phenylhydrazine-carbothioamide (**5b**), the respective α-halogenated ketone and 2-propanol. The reaction mixture was kept under magnetic stirring, at room temperature, for 1 h. The reactions were followed by thin layer chromatographic plate. The formed precipitate was filtered on sintered funnel with distilled water, yielding the pure product.

4.1.5.1. 2-((*E*)-2-((*Z*)-[3,4-diphenylthiazol-2(3*H*)-ylidene]hydrazono)ethyl)isoindoline-1,3-dione (**6b**). Orange crystals; Yield: 56%; m.p. (°C) 196–198; Rf 0.46 (hexane/ethyl acetate 3:2); IR (KBr, cm⁻¹): 1712.40 (C=O). ¹H NMR (300 MHz, DMSO-*d*₆), δ ppm: 4.42 (d, *J* = 3 Hz 2H, CH₂), 6.45 (s, 1H, CH, thiazole), 7.09–7.32 (m, 10H, CH Ar), 7.44 (t, *J* = 3 Hz, 1H, HC=N), 7.91–7.88 (m, 4H, CH Ar, phthalimide); ¹³C NMR (75.5 MHz, DMSO-*d*₆), δ ppm: 40.3 (CH₂), 104.2 (CH, thiazole), 123.0 (Ar), 125.2 (Ar), 128.0 (Ar), 128.1 (Ar), 128.3 (Ar), 128.6 (Ar), 128.8 (Ar), 130.6 (Ar), 131.8 (Ar), 134.4 (Ar), 137.3 (Ar), 139.3 (C, thiazole), 148.2 (C=N), 167.5 (C=O), 169.9 (S–C–N, thiazole). Anal. Calcd for C₂₅H₁₈N₄O₂S: C, 68.48; H, 4.14; N, 12.78; S, 7.31. found: C, 66.88; H, 4.30; N, 12.48; S, 7.12. HRMS: 439.1028 [M+H]⁺.

4.1.5.2. 2-((*E*)-2-((*Z*)-[3-phenyl-4-*p*-tolylthiazol-2(3*H*)-ylidene]hydrazono)ethyl)isoindoline-1,3-dione (**6c**). Yellow crystals; Yield: 52%; m.p. (°C) 156–158; Rf: 0.7 (hexane/ethyl acetate 3:2). IR (KBr, cm⁻¹): 1712.39 (C=O). ¹H NMR (300 MHz, DMSO-*d*₆), δ ppm: 2.19 (s, 3H, CH₃), 4.42 (d, *J* = 3 Hz, 2H, CH₂), 6.41 (s, 1H, CH thiazole), 6.95–6.99 (m, 4H, CH Ar), 7.17–7.45 (m, 6H, CH Ar), 7.88–7.95 (m, 4H, CH Ar phthalimide); ¹³C NMR (75.5 MHz, DMSO-*d*₆), δ ppm: 20.7 (CH₃), 38.9 (CH₂), 100.7 (CH, thiazole), 123.1 (Ar), 127.7 (Ar), 128.1 (Ar), 128.7 (Ar), 128.8 (Ar), 128.9 (Ar), 129.8 (Ar), 131.8 (Ar), 134.5 (Ar), 137.4 (Ar), 137.9 (Ar), 139.456 (C, thiazole), 148.2 (C=N), 167.6 (C=O), 170.1 (S–C–N, thiazole). Anal. Calcd for C₂₆H₂₀N₄O₂S: C, 69.01; H, 4.45; N, 12.38; S, 7.09. found: C, 68.66; H, 4.36; N, 12.12; S, 6.96. HRMS: 453.1138 [M+H]⁺.

4.1.5.3. 2-((*E*)-2-((*Z*)-[4-(4-methoxyphenyl)-3-phenylthiazol-2(3*H*)-ylidene]hydrazono)ethyl)isoindoline-1,3-dione (**6d**). Yellow crystals; Yield: 54%; m.p. (°C) 173–175; Rf 0.49 (hexane/ethyl acetate 3:2); IR (KBr, cm⁻¹): 1713.83 (C=O). ¹H NMR (300 MHz, DMSO-*d*₆), δ ppm: 4.18 (s, 3H, CH₃), 4.44 (d, *J* = 3 Hz, 2H, CH₂), 6.83–8.10 (m, 14H, Ar); ¹³C NMR (75.5 MHz, DMSO-*d*₆), δ ppm: 40.1 (CH₂), 56.4 (CH₃), 104.3 (CH, thiazole), 123.1 (Ar), 123.3 (Ar), 127.9 (Ar), 128.4 (Ar), 128.8 (Ar), 129.2 (Ar), 131.7 (Ar), 134.5 (Ar), 136.6 (Ar), 136.7 (Ar), 137.6 (Ar), 139.0 (C, thiazole), 146.8 (C=N), 167.5 (C=O), 169.6 (S–C–N, thiazole). Anal. Calcd for C₂₆H₂₀N₄O₃S: C, 66.65; H, 4.30; N, 11.96; S, 6.84. found: C, 65.60; H, 4.08; N, 11.85; S, 6.68. HRMS: 469.1276 [M+H]⁺.

4.1.5.4. 2-((*E*)-2-((*Z*)-[4-(4-fluorophenyl)-3-phenylthiazol-2(3*H*)-ylidene]hydrazono)ethyl)isoindoline-1,3-dione (**6e**). Yellow crystals; Yield: 50%; m.p. (°C) 176–179; Rf: 0.63 (hexane/ethyl acetate 3:2); IR (KBr, cm⁻¹): 1714.47 (C=O); ¹H NMR (300 MHz, DMSO-*d*₆), δ ppm: 4.43 (d, *J* = 3 Hz, 2H, CH₂), 6.47 (s, 1H, CH thiazole), 7.02–7.36 (m, 9H, CH Ar), 7.45 (t, *J* = 3 Hz, 1H, CH), 7.86–7.95 (m, 4H, CH Ar phthalimide); ¹³C NMR (75.5 MHz, DMSO-*d*₆), δ ppm: 38.9 (CH₂), 101.3 (CH, thiazole), 115.1 (Ar), 115.3 (Ar), 123.1 (Ar), 127.1 (Ar), 128.0 (Ar), 128.7 (Ar), 128.9 (Ar), 130.6 (Ar), 131.8 (Ar), 134.5 (Ar), 137.2 (Ar), 138.3 (C, thiazole), 148.3 (C=N), 160.2 and 163.4 (C–F), 167.6

(C=O), 169.9 (S–C–N, thiazole). Anal. Calcd for C₂₅H₁₇FN₄O₂S: C, 65.78; H, 3.75; N, 12.27; S, 7.02. found: C, 63.91; H, 3.79; N, 12.01; S, 6.94. HRMS: 457.1083 [M+H]⁺.

4.1.5.5. 2-((Z)-[4-(4-chlorophenyl)-3-phenylthiazol-2(3H)-ylidene]hydrazono)ethylisoindoline-1,3-dione (**6f**). Yellow crystals; Yield: 58%; m.p. (°C) 176–179; Rf: 0.84 (hexane/ethyl acetate 3:2); IR (KBr, cm⁻¹): 1717.30 (C=O). ¹H NMR (300 MHz, DMSO-*d*₆), δ_{ppm}: 4.41 (d, *J* = 3 Hz, 2H, CH₂), 6.50 (s, 1H, thiazole), 7.07–7.37 (m, 9H, Ar), 7.44 (t, *J* = 3 Hz, 1H) 7.85–7.94 (m, 5H, Ar); ¹³C NMR (75.5 MHz, DMSO-*d*₆), δ_{ppm}: 56.0 (CH₂), 101.8 (CH, thiazole), 123.1 (Ar), 127.9 (Ar), 128.1 (Ar), 128.6 (Ar), 128.9 (Ar), 129.5 (Ar), 129.9 (Ar), 131.8 (Ar), 133.1 (Ar), 134.5 (Ar), 137.2 (Ar), 138.7 (C, thiazole), 148.3 (C=N), 167.6 (C=O), 169.9 (S–C–N, thiazole). Anal. Calcd for C₂₅H₁₇ClN₄O₂S: C, 63.49; H, 3.62; N, 11.85; S, 6.78. found: C, 61.17; H, 3.43; N, 11.47; S, 6.79. HRMS: 473.0793 [M+H]⁺.

4.1.5.6. 2-((E)-2-((Z)-[4-(4-bromophenyl)-3-phenylthiazol-2(3H)-ylidene]hydrazono)ethyl)isoindoline-1,3-dione (**6g**). White crystals; Yield: 55%; m.p. (°C) 189–193; Rf: 0.73 (hexane/ethyl acetate 3:2); IR (KBr, cm⁻¹): 1717.05 (C=O). ¹H NMR (300 MHz, DMSO-*d*₆), δ_{ppm}: 4.42 (d, *J* = 3 Hz, 2H, CH₂), 6.51 (s, 1H, thiazole), 7.01–7.94 (m, 14H, Ar); ¹³C NMR (75.5 MHz, DMSO-*d*₆), δ_{ppm}: 39.3 (CH₂), 101.87 (CH, thiazole), 121.7 (Ar), 123.1 (Ar), 127.9 (Ar), 128.6 (Ar), 128.9 (Ar), 129.8 (Ar), 130.1 (Ar), 131.2 (Ar), 131.8 (Ar), 134.5 (Ar), 137.2 (Ar), 138.1 (C, thiazole), 148.5 (C=N), 167.6 (C=O), 169.9 (S–C–N, thiazole). Anal. Calcd for C₂₅H₁₇BrN₄O₂S: C, 58.03; H, 3.31; N, 10.83; S, 6.20. found: C, 57.27; H, 3.28; N, 10.68; S, 6.06. HRMS: 517.0005 [M+H]⁺.

4.1.5.7. 2-((E)-2-((Z)-[4-(4-nitrophenyl)-3-phenylthiazol-2(3H)-ylidene]hydrazono)ethyl)isoindoline-1,3-dione (**6h**). Orange crystals; Yield: 46%; m.p. (°C) 186–189; Rf: 0.75 (hexane/ethyl acetate 3:2). IR (KBr, cm⁻¹): 1713.38 (C=O). ¹H NMR (300 MHz, DMSO-*d*₆), δ_{ppm}: 4.45 (d, *J* = 3 Hz, 2H, CH₂), 6.78–8.10 (m, 15H, Ar); ¹³C NMR (75.5 MHz, DMSO-*d*₆), δ_{ppm}: 40.1 (CH₂), 102.0 (CH, thiazole), 123.2 (Ar), 123.3 (Ar), 124.5 (Ar), 128.0 (Ar), 128.4 (Ar), 129.0 (Ar), 131.7 (Ar), 131.7 (Ar), 134.5 (Ar), 136.7 (Ar), 137.4 (Ar), 138.7 (C, thiazole), 146.7 (C=N), 167.5 (C=O), 169.6 (S–C–N, thiazole). Anal. Calcd for C₂₅H₁₇N₅O₄S: C, 62.10; H, 3.54; N, 14.48; S, 6.63. found: C, 59.19; H, 3.65; N, 13.76; S, 6.93. HRMS: 484.0975 [M+H]⁺.

4.1.5.8. 2-((E)-2-((Z)-[4-(biphenyl-4-yl)-3-phenylthiazol-2(3H)-ylidene]hydrazono)ethyl)isoindoline-1,3-dione (**6i**). Yellow crystals; Yield: 73%; m.p. (°C) 157–159; Rf: 0.43 (hexane/ethyl acetate 3:2); IR (KBr, cm⁻¹): 1716.38 (C=O). ¹H NMR (400 MHz, DMSO-*d*₆), δ_{ppm}: 4.48 (d, *J* = 3.6 Hz, 2H, CH₂), 6.05 (s, 1H, thiazole), 7.00–7.82 (m, 19H, Ar); ¹³C NMR (75.5 MHz, DMSO-*d*₆), δ_{ppm}: 39.2 (CH₂), 101.2 (CH, thiazole), 123.3 (Ar), 126.8 (Ar), 126.9 (Ar), 127.7 (Ar), 128.3 (Ar), 128.4 (Ar), 128.5 (Ar), 128.6 (Ar), 128.7 (Ar), 128.8 (Ar), 129.2 (Ar), 129.6 (Ar), 132.3 (Ar), 133.9 (Ar), 133.9 (Ar), 139.9 (C, thiazole), 141.2 (C=N), 167.8 (C=O), 169.0 (S–C–N, thiazole). Anal. Calcd for C₃₁H₂₂N₄O₂S: C, 72.35; H, 4.31; N, 10.89; S, 6.23. found: C, 70.19; H, 4.32; N, 10.35; S, 6.53. HRMS: 515.1416 [M+H]⁺.

4.1.5.9. 2-((E)-2-((Z)-[4-(naphthalen-2-yl)-3-phenylthiazol-2(3H)-ylidene]hydrazono)ethyl)isoindoline-1,3-dione (**6j**). Yellow crystals; Yield: 68%; m.p. (°C) 159–161; Rf: 0.43 (hexane/ethyl acetate 3:2); IR (KBr, cm⁻¹): 1713.93 (C=O). ¹H NMR (400 MHz, DMSO-*d*₆), δ_{ppm}: 4.56 (d, *J* = 4 Hz, 2H, CH₂), 6.18 (s, 1H, thiazole), 6.99–7.91 (m, 17H, Ar); ¹³C NMR (75.5 MHz, DMSO-*d*₆), δ_{ppm}: 39.2 (CH₂), 101.6 (CH, thiazole), 123.3 (Ar), 125.4 (Ar), 126.5 (Ar), 126.7 (Ar), 127.6 (Ar), 127.7 (Ar), 127.8 (Ar), 128.0 (Ar), 128.1 (Ar), 128.3 (Ar), 128.4 (Ar), 128.7 (Ar), 129.2 (Ar), 132.3 (Ar), 132.8 (Ar), 133.9 (Ar), 137.5 (Ar), 140.3 (C, thiazole), 149.5 (C=N), 167.8 (C=O), 171.0 (S–C–N,

thiazole). Anal. Calcd for C₂₉H₂₀N₄O₂S: C, 71.29; H, 4.13; N, 11.47; S, 6.56. found: C, 70.09; H, 4.21; N, 11.41; S, 6.70. HRMS: 489.1296 [M+H]⁺.

4.1.5.10. 2-((E)-2-((Z)-[4-(3-nitrophenyl)-3-phenylthiazol-2(3H)-ylidene]hydrazono)ethyl)isoindoline-1,3-dione (**6k**). Yellow crystals; Yield: 63%; m.p. (°C) 154–154; Rf: 0.34 (hexane/ethyl acetate 3:2); IR (KBr, cm⁻¹): 1712.80 (C=O). ¹H NMR (300 MHz, DMSO-*d*₆), δ_{ppm}: 4.43 (d, *J* = 2.7 Hz, 2H, CH₂), 6.76 (s, 1H, CH thiazole), 7.25–7.38 (m, 5H, CH Ar), 7.48–7.51 (m, 3H, CH Ar), 7.86–7.95 (m, 6H, CH Ar), 8.07 (t, *J* = 2.4 Hz, 1H, HC=N); ¹³C NMR (75.5 MHz, DMSO-*d*₆), δ_{ppm}: 39.3 (CH₂), 104.3 (CH, thiazole), 123.2 (Ar), 123.4 (Ar), 123.6 (Ar), 128.8 (Ar), 128.9 (Ar), 129.1 (Ar), 129.3 (Ar), 129.5 (Ar), 129.6 (Ar), 130.0 (Ar), 130.3 (Ar), 135.0 (Ar), 135.6 (Ar), 138.8 (C, thiazole), 149.3 (C=N), 167.5 (C=O), 169.6 (S–C–N, thiazole). Anal. Calcd for C₂₅H₁₇N₅O₄S: C, 62.10; H, 3.54; N, 14.48; S, 6.63. found: C, 60.45; H, 3.70; N, 14.10; S, 6.48. HRMS: 484.0976 [M+H]⁺.

4.1.5.11. 2-((E)-2-((Z)-[4-(3,4-dichlorophenyl)-3-phenylthiazol-2(3H)-ylidene]hydrazono)ethyl)isoindoline-1,3-dione (**6l**). Yellow crystals; Yield: 48%; m.p. (°C) 155–157; Rf: 0.89 (hexane/ethyl acetate 3:2); IR (KBr, cm⁻¹): 1714.45 (C=O). ¹H NMR (300 MHz, DMSO-*d*₆), δ_{ppm}: 4.45 (d, *J* = 3 Hz, 2H, CH₂), 6.81–7.92 (m, 14H, Ar); ¹³C NMR (75.5 MHz, DMSO-*d*₆), δ_{ppm}: 40.1 (CH₂), 104.6 (CH, thiazole), 123.1 (Ar), 128.3 (Ar), 128.6 (Ar), 128.9 (Ar), 129.3 (Ar), 130.3 (Ar), 130.5 (Ar), 130.9 (Ar), 131.4 (Ar), 131.7 (Ar), 134.3 (Ar), 134.6 (Ar), 136.1 (Ar), 137.3 (C, thiazole), 149.2 (C=N), 167.5 (C=O), 169.6 (S–C–N, thiazole); Anal. Calcd for C₂₅H₁₆Cl₂N₄O₂S: C, 59.18; H, 3.18; N, 11.04; S, 6.32. found: C, 56.85; H, 3.30; N, 10.58; S, 6.02. HRMS: 507.0432 [M+H]⁺.

4.2. X-ray analysis

X-ray diffraction data collections were performed on an Enraf-Nonius Kappa-CCD diffractometer (95 mm CCD camera on κ-goniostat) using graphite monochromated MoKα radiation (0.71073 Å) at room temperature. Data were collected using the COLLECT software [37] up to 50° (2θ). The final unit cell parameters were based on 15666, 9327, and 12333 reflections as well as the corrections for Lorentz and polarization effects were performed with the HKL DENZO-SCALEPACK system of programs [38]. The compound structures were solved by direct methods with SHELXS-97 [39]. The model was refined by full-matrix least squares on F₂ using SHELXL-97 [39]. The program ORTEP-3 [40] was used for graphic representations, and the program WinGX [41] was used to prepare the material for publication. All H atoms were located by geometric considerations placed (C–H = 0.93 Å; N–H = 0.86 Å) and refined using a riding model with Uiso(H) = 1.5Ueq(C-methyl) or 1.2Ueq(other). An Ortep-3 diagram of the molecules is shown in Fig. 2, and Table S1 shows the main crystallographic data. Crystallographic data (excluding structure factors) for the structures reported in this paper have been deposited with the Cambridge Crystallographic Data Centre as supplementary material (No. CCDC 1411254, 1411262 and 1411263).

4.3. Biological assays of toxicity to splenocytes

Splenocytes from BALB/c mice were divided into a 96 well plate at a density of 5 × 10⁶ cells per well in RPMI-1640 medium containing 10% inactivated Foetal Bovine Serum (FBS). Each chemical inhibitor was dissolved in DMSO at a concentration of 10 mg/mL, and then the sample was serially diluted in RPMI-1640 medium supplemented with 10% FBS at concentrations of 1.0, 5.0, 10, 25, 50 and 100 µg/mL, in triplicate. As a positive control, saponin was used

at a concentration of 0.1 µg/mL, while RPMI-1640 medium supplemented with 10% FBS and DMSO was used as a negative control. A total of 1.0 µCi of 3H-thymidine was added to each well, and the plate was incubated for 24 h at 37 °C and 5% CO₂.

The plate was then read in the counter beta irradiation reader (Multilabel Reader, Finland), and the percent incorporation of tritiated thymidine was determined. Cells that were not treated with drugs (negative controls) were calculated as 100% of tritiated thymidine incorporation (100% viable cells). For cells treated with saponin, cell viability was 5%. When the percentage of incorporation was higher than 90%, the concentration of the drug was regarded as nontoxic to splenocytes.

4.4. Antiproliferative activity for the epimastigote form

Epimastigotes of Dm28c strain were distributed into a 96 well plate to a final density of 10⁶ cells per well. Each chemical inhibitor was dissolved in the respective wells, in triplicate. Benznidazole was used as positive controls in this assay. The plate was then cultivated for 4 days at 27 °C. After this time, aliquots from each well were collected, and the number of parasites was calculated in a Neubauer chamber. Epimastigotes not treated with the chemical inhibitors (negative control) were assumed as 100% the number of parasites. The dose–response curves were determined, and the IC₅₀ values were calculated using at least five concentrations (data points) and a nonlinear equation (Prism, version 4.0).

4.5. Toxicity to trypomastigotes

Strain Y trypomastigotes were collected from Vero cell supernatants and distributed in a 96 well plate to a final density of 4 × 10⁵ cells per well. Each chemical inhibitor was added to the wells, in triplicate. Benznidazole was used as positive controls in this assay. The plate was then cultivated for 24 h at 37 °C and 5% CO₂. After this time, aliquots from each well were collected, and the number of viable parasites (i.e., with apparent motility) was counted in a Neubauer chamber. The wells that did not receive the chemical inhibitors were assumed as 100% the number of viable parasites. The dose–response curves were determined, and the IC₅₀ values were calculated by nonlinear regression (Prism, version 4.0) using at least seven concentrations (data points).

4.6. Ultrastructural studies

The parasites were cultured for 24 h in RPMI 1640 medium (Sigma–Aldrich, St. Louis, MO, USA) buffered to pH 7.5 and supplemented with HEPES (20 mM), 10% foetal bovine serum, penicillin (100 U/mL), and streptomycin (100 µg/mL) containing the compound **6k** at the IC₅₀ concentration and twice the value of IC₅₀. The parasites were collected, washed in PBS and fixed with 2.5% glutaraldehyde, 4% formaldehyde, and 0.1 M cacodylate buffer at pH 6.8. They were then postfixed in 2% osmium tetroxide (OsO₄) in a 0.1 M cacodylate buffer at pH 6.8 and processed for routine transmission electron microscopy (TEM) and scanning electron microscopy (SEM).

For SEM analysis, the parasites were dehydrated in graded ethanol and dried by the critical point method with CO₂. The samples were mounted on aluminium stubs, coated with gold and examined under a JEOL-5600LV microscope.

For TEM analysis, the parasites were dehydrated in a graded series of acetone and finally embedded in epon. Sections were stained with uranyl acetate and lead citrate and observed with Tecnai spirit G2 Biotwin microscope.

4.7. Propidium iodide and annexin V staining

Trypomastigotes (1 × 10⁷) were incubated for 24 h at 37 °C in the absence or presence of compound **6k**. After incubation, the parasites were labelled with propidium iodide (PI) and annexin V using the annexin V-FITC apoptosis detection kit (Sigma–Aldrich), according to the manufacturer's instructions. Acquisition and analyses were performed using a FACS Calibur flow cytometer (Becton Dickinson, CA, USA) with FlowJo software (Tree Star, CA, USA). A total of 30,000 events were acquired in the region previously established as trypomastigote forms of *T. cruzi*. Two independent experiments were performed.

Acknowledgements

This work was funded by Conselho Nacional de Desenvolvimento Científico e Tecnológico (CNPq), Fundação de Amparo à Ciência e Tecnologia de Pernambuco (FACEPE, APQ-0549-2.11/14, APQ-0289-4.03/13). P.A.T.M.G. holds a FACEPE doctoral scholarship. Authors are thankful to the Departamento de Química Fundamental (DQF-UFPE) for recording the ¹H NMR, ¹³C NMR, LCMS and IR spectra of compounds. We are also thankful to Julia Campos of Centro de Tecnologias Estratégicas do Nordeste (CETENE) for recording the MS spectra of compounds **6a–l**. All authors declare no competing financial interest.

Appendix A. Supplementary data

Supplementary data related to this article can be found at <http://dx.doi.org/10.1016/j.ejmech.2016.01.010>.

References

- [1] WHO, Chagas Disease (American Trypanosomiasis), 2015. <http://www.who.int/mediacentre/factsheets/fs340/en/index.html>.
- [2] J. Urbina, Chemotherapy of chagas disease, *Curr. Pharm. Des.* 8 (2002) 287–295, <http://dx.doi.org/10.2174/1381612023396177>.
- [3] Ja Pérez-Molina, J. Sojo-Dorado, F. Norman, B. Monge-Maillo, M. Díaz-Menéndez, P. Albajar-Viñas, et al., Nifurtimox therapy for chagas disease does not cause hypersensitivity reactions in patients with such previous adverse reactions during benznidazole treatment, *Acta Trop.* 127 (2013) 101–104, <http://dx.doi.org/10.1016/j.actatropica.2013.04.003>.
- [4] M.V. de O. Cardoso, L.R.P. de Siqueira, E.B. da Silva, L.B. Costa, M.Z. Hernandez, M.M. Rabello, et al., 2-pyridyl thiazoles as novel anti- Trypanosoma cruzi agents : structural design, synthesis and pharmacological evaluation, *Eur. J. Med. Chem.* 86 (2014) 48–59, <http://dx.doi.org/10.1016/j.ejmech.2014.08.012>.
- [5] S.S. Gawande, S.C. Warangkar, B.P. Bandgar, C.N. Khobragade, Synthesis of new heterocyclic hybrids based on pyrazole and thiazolidinone scaffolds as potent inhibitors of tyrosinase, *Bioorg. Med. Chem.* 21 (2013) 2772–2777, <http://dx.doi.org/10.1016/j.bmc.2012.12.053>.
- [6] G.N. Masoud, A.M. Youssef, M.M. Abdel Khalek, A.E. Abdel Wahab, I.M. Labouta, A.a.B. Hazzaa, Design, synthesis, and biological evaluation of new 4-thiazolidinone derivatives substituted with benzimidazole ring as potential chemotherapeutic agents, *Med. Chem. Res.* 22 (2012) 707–725, <http://dx.doi.org/10.1007/s00044-012-0057-3>.
- [7] D.R.M. Moreira, S.P.M. Costa, M.Z. Hernandez, M.M. Rabello, G.B. de Oliveira Filho, C.M.L. de Melo, et al., Structural investigation of anti-Trypanosoma cruzi 2-iminothiazolidin-4-ones allows the identification of agents with efficacy in infected mice, *J. Med. Chem.* 55 (2012) 10918–10936, <http://dx.doi.org/10.1021/jm301518v>.
- [8] C. Pizzo, C. Saiz, A. Talevi, L. Gavernet, P. Palestro, C. Bellera, et al., Synthesis of 2-hydrazolyl-4-thiazolidinones based on multicomponent reactions and biological evaluation against Trypanosoma Cruzi, *Chem. Biol. Drug Des.* 77 (2011) 166–172, <http://dx.doi.org/10.1111/j.1747-0285.2010.01071.x>.
- [9] M.E. Caputto, A. Ciccarelli, F. Frank, A.G. Moglioni, G.Y. Moltrasio, D. Vega, et al., Synthesis and biological evaluation of some novel 1-indanone thiazolylhydrazone derivatives as anti-Trypanosoma cruzi agents, *Eur. J. Med. Chem.* 55 (2012) 155–163, <http://dx.doi.org/10.1016/j.ejmech.2012.07.013>.
- [10] M.Z. Hernandez, M.M. Rabello, A.C.L. Leite, M.V.O. Cardoso, D.R.M. Moreira, D.J. Brondani, et al., Studies toward the structural optimization of novel thiazolylhydrazone-based potent antitrypanosomal agents, *Bioorg. Med. Chem.* 18 (2010) 7826–7835, <http://dx.doi.org/10.1016/j.bmc.2010.09.056>.
- [11] A.C.L. Leite, R.S. de Lima, D.R.D.M. Moreira, M.V.D.O. Cardoso, A.C. Gouveia de Brito, L.M. Farias Dos Santos, et al., Synthesis, docking, and in vitro activity of

- thiosemicarbazones, aminoacyl-thiosemicarbazides and acyl-thiazolidones against *Trypanosoma cruzi*, *Bioorg. Med. Chem.* 14 (2006) 3749–3757, <http://dx.doi.org/10.1016/j.bmc.2006.01.034>.
- [12] A.C.L. Leite, D.R. de M. Moreira, M.V. de O. Cardoso, M.Z. Hernandez, V.R. Alves Pereira, R.O. Silva, et al., Synthesis, Cruzain docking, and in vitro studies of aryl-4-oxothiazolylhydrazones against *Trypanosoma cruzi*, *Chem. Med. Chem.* 2 (2007) 1339–1345, <http://dx.doi.org/10.1002/cmdc.200700022>.
- [13] J.W.P. Espíndola, M.V. de O. Cardoso, G.B. de O. Filho, D.A. Oliveira e Silva, D.R.M. Moreira, T.M. Bastos, et al., Synthesis and structure–activity relationship study of a new series of antiparasitic aryloxy thiosemicarbazones inhibiting *Trypanosoma cruzi* cruzain, *Eur. J. Med. Chem.* 101 (2015) 818–835, <http://dx.doi.org/10.1016/j.ejmech.2015.06.048>.
- [14] G.B. de Oliveira Filho, M.V. de Oliveira Cardoso, J.W.P. Espíndola, L.F.G.R. Ferreira, C.A. de Simone, R.S. Ferreira, et al., Structural design, synthesis and pharmacological evaluation of 4-thiazolidinones against *Trypanosoma cruzi*, *Bioorg. Med. Chem.* 23 (2015) 7478–7486, <http://dx.doi.org/10.1016/j.bmc.2015.10.048>.
- [15] A.M. Alanazi, A.S. El-Azab, I.A. Al-Suwaidan, K.E.H. ElTahir, Y.A. Asiri, N.I. Abdel-Aziz, et al., Structure-based design of phthalimide derivatives as potential cyclooxygenase-2 (COX-2) inhibitors: anti-inflammatory and analgesic activities, *Eur. J. Med. Chem.* 92 (2015) 115–123, <http://dx.doi.org/10.1016/j.ejmech.2014.12.039>.
- [16] K. Kamiński, J. Obniska, B. Wiklik, D. Atamanyuk, Synthesis and anticonvulsant properties of new acetamide derivatives of phthalimide, and its saturated cyclohexane and norbornene analogs, *Eur. J. Med. Chem.* 46 (2011) 4634–4641, <http://dx.doi.org/10.1016/j.ejmech.2011.07.043>.
- [17] H. Akgün, İ. Karamelekoğlu, B. Berk, I. Kurnaz, G. Sarıbiyık, S. Öktem, et al., Synthesis and antimycobacterial activity of some phthalimide derivatives, *Bioorg. Med. Chem.* 20 (2012) 4149–4154, <http://dx.doi.org/10.1016/j.bmc.2012.04.060>.
- [18] A.A.-M. Abdel-Aziz, A.S. El-Azab, S.M. Attia, A.M. Al-Obaid, M.A. Al-Omar, H.I. El-Subbagh, Synthesis and biological evaluation of some novel cyclic imides as hypoglycaemic, anti-hyperlipidemic agents, *Eur. J. Med. Chem.* 46 (2011) 4324–4329, <http://dx.doi.org/10.1016/j.ejmech.2011.07.002>.
- [19] G. Singh, A. Saroa, S. Girdhar, S. Rani, S. Sahoo, D. Choquesillo-Lazarte, Synthesis, characterization, electronic absorption and antimicrobial studies of N-(silyltranylpropyl)phthalimide derived from phthalic anhydride, *Inorganica Chim. Acta* 427 (2015) 232–239, <http://dx.doi.org/10.1016/j.jca.2015.01.011>.
- [20] K. Elumalai, M.A. Ali, M. Elumalai, K. Eluri, S. Srinivasan, S. Sivannan, et al., Synthesis, characterization and biological evaluation of acetazolamide, cycloserine and isoniazid condensed some novel phthalimide derivatives, *Int. J. Chem. Anal. Sci.* 4 (2013) 57–61, <http://dx.doi.org/10.1016/j.ijcas.2013.04.004>.
- [21] R. Williams, J.T. Manka, A.L. Rodriguez, P.N. Vinson, C.M. Niswender, C.D. Weaver, et al., Synthesis and SAR of centrally active mGlu5 positive allosteric modulators based on an aryl acetylenic bicyclic lactam scaffold, *Bioorg. Med. Chem. Lett.* 21 (2011) 1350–1353, <http://dx.doi.org/10.1016/j.bmcl.2011.01.044>.
- [22] A.C.L. Leite, F.F. Barbosa, M.V.D.O. Cardoso, D.R.M. Moreira, L.C.D. Coelho, E.B. Silva, et al., Phthaloyl amino acids as anti-inflammatory and immunomodulatory prototypes, *Med. Chem. Res.* (2013), <http://dx.doi.org/10.1007/s00044-013-0730-1>.
- [23] M.V.D.O. Cardoso, D.R.M. Moreira, G.B.O. Filho, S.M.T. Cavalcanti, L.C.D. Coelho, J.W.P. Espíndola, et al., Design, synthesis and structure–activity relationship of phthalimides endowed with dual antiproliferative and immunomodulatory activities, *Eur. J. Med. Chem.* 96 (2015) 491–503, <http://dx.doi.org/10.1016/j.ejmech.2015.04.041>.
- [24] L.C.D. Coelho, M.V. de O. Cardoso, D.R.M. Moreira, P.A.T. de M. Gomes, S.M.T. Cavalcanti, A.R. Oliveira, et al., Novel phthalimide derivatives with TNF- α and IL-1 β expression inhibitory and apoptotic inducing properties, *Medchemcomm* 5 (2014) 758, <http://dx.doi.org/10.1039/c4md00070f>.
- [25] C. Pessoa, P.M.P. Ferreira, L.V.C. Lotufo, M.O. de Moraes, S.M.T. Cavalcanti, L.C.D. Coelho, et al., Discovery of phthalimides as immunomodulatory and antitumor drug prototypes, *Chem. Med. Chem.* 5 (2010) 523–528, <http://dx.doi.org/10.1002/cmdc.200900525>.
- [26] P.M. da Costa, M.P. da Costa, A.A. Carvalho, S.M.T. Cavalcanti, M.V. de Oliveira Cardoso, G.B. de Oliveira Filho, et al., Improvement of in vivo anticancer and antiangiogenic potential of thalidomide derivatives, *Chem. Biol. Interact.* 239 (2015) 174–183, <http://dx.doi.org/10.1016/j.cbi.2015.06.037>.
- [27] E. de F. Santiago, S.A. de Oliveira, G.B. de Oliveira Filho, D.R.M. Moreira, P.A.T. Gomes, A.C.L.A.C.L. da Silva, et al., Evaluation of the anti-schistosoma mansoni activity of Thiosemicarbazones and Thiazoles, *Antimicrob. Agents Chemother.* 58 (2014) 352–363, <http://dx.doi.org/10.1128/AAC.01900-13>.
- [28] M. Cardoso, M. Hernandez, D. Moreira, F. Pontes, C. Simone, A. Leite, Structural insights into bioactive Thiazolidin-4-one: experimental and theoretical data, *Lett. Org. Chem.* 12 (2015) 262–270, <http://dx.doi.org/10.2174/1570178612666150203005612>.
- [29] D.R.M. Moreira, A.C. Lima Leite, M.V.O. Cardoso, R.M. Srivastava, M.Z. Hernandez, M.M. Rabello, et al., Structural design, synthesis and structure–activity relationships of thiazolidinones with enhanced anti-trypanosoma cruzi activity, *Chem. Med. Chem.* 9 (2014) 177–188, <http://dx.doi.org/10.1002/cmdc.201300354>.
- [30] M. Congreve, R. Carr, C. Murray, H. Jhoti, A “Rule of Three” for fragment-based lead discovery? *Drug Discov. Today* 8 (2003) 876–877, [http://dx.doi.org/10.1016/S1359-6446\(03\)02831-9](http://dx.doi.org/10.1016/S1359-6446(03)02831-9).
- [31] H. Chen, X. Zhou, A. Wang, Y. Zheng, Y. Gao, J. Zhou, Evolutions in fragment-based drug design: the deconstruction–reconstruction approach, *Drug Discov. Today* 20 (2015) 105–113, <http://dx.doi.org/10.1016/j.drudis.2014.09.015>.
- [32] M. Gonzales-Perdomo, S.L. de Castro, M.N. Meirelles, S. Goldenberg, *Trypanosoma cruzi* proliferation and differentiation are blocked by topoisomerase II inhibitors, *Antimicrob. Agents Chemother.* 34 (1990) 1707–1714, <http://dx.doi.org/10.1128/AAC.34.9.1707>.
- [33] E.M. De Souza, A. Lansiaux, C. Bailly, W.D. Wilson, Q. Hu, D.W. Boykin, et al., Phenyl substitution of furamide markedly potentiates its anti-parasitic activity against *trypanosoma cruzi* and *Leishmania amazonensis*, *Biochem. Pharmacol.* 68 (2004) 593–600, <http://dx.doi.org/10.1016/j.bcp.2004.04.019>.
- [34] L.R. Garzoni, A. Caldera, M. de N.L. Meirelles, S.L.D. Castro, R. Docampo, G.A. Meints, et al., Selective in vitro effects of the farnesyl pyrophosphate synthase inhibitor risedronate on *trypanosoma cruzi*, *Int. J. Antimicrob. Agents* 23 (2004) 273–285, <http://dx.doi.org/10.1016/j.ijantimicag.2003.07.020>.
- [35] M.V. Braga, J.A. Urbina, W. de Souza, Effects of squalene synthase inhibitors on the growth and ultrastructure of *trypanosoma cruzi*, *Int. J. Antimicrob. Agents* 24 (2004) 72–78, <http://dx.doi.org/10.1016/j.ijantimicag.2003.12.009>.
- [36] A.P. Dantas, K. Salomão, H.S. Barbosa, S.L. De Castro, The effect of Bulgarian propolis against *trypanosoma cruzi* and during its interaction with host cells, *Mem. Inst. Oswaldo Cruz* 101 (2006) 207–211, <http://dx.doi.org/10.1590/S0074-02762006000200013>.
- [37] E.-N. Collect, Nonius BV, Delft, The Netherlands. 2000 (1997) 585.
- [38] Z. Otwinowski, W. Minor, Methods in enzymology, *Macromol. Crystallogr. Part A* 276 (1997) 307–326, [http://dx.doi.org/10.1016/S0076-6879\(97\)76066-X](http://dx.doi.org/10.1016/S0076-6879(97)76066-X).
- [39] G. Sheldrick, SHELXL-97 and SHELXS-97, Program for X-ray Crystal Structure Solution and Refinement, Univ. Göttingen, 1997. <http://scholar.google.com.br/scholar?q=SHELXS-97:Program for Crystal Structure Resolution#3>.
- [40] L.J. Farrugia, ORTEP -3 for Windows - a version of ORTEP -III with a Graphical User interface (GUI), *J. Appl. Crystallogr.* 30 (1997) 565, <http://dx.doi.org/10.1107/S0021889897003117>.
- [41] L.J. Farrugia, WinGX suite for small-molecule single-crystal crystallography, *J. Appl. Crystallogr.* 32 (1999) 837–838, <http://dx.doi.org/10.1107/S0021889899006020>.